Tight Symmetry Energy Parameter Constraints from Neutron Skin Measurements

J. M. Lattimer

Department of Physics & Astronomy

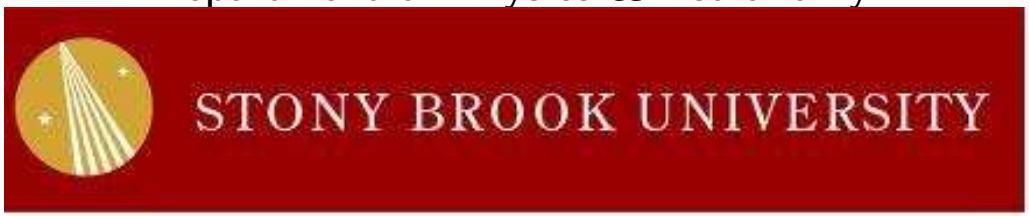

U.S. DEPARTMENT OF ENERGY

Office of Science

SINT Seminar

INT, Seattle, WA, March 14, 2023

Acknowledgements

Funding Support:

DOE - Nuclear Physics

DOE - Toward Exascale Astrophysics of Mergers and Supernovae (TEAMS)

NASA - Neutron Star Interior Composition ExploreR (NICER)

NSF - Neutrinos, Nuclear Astrophysics and Symmetries (PFC - N3AS)

DOE - Nuclear Physics from Multi-Messenger Mergers (NP3M)

Recent Collaborators:

Duncan Brown & Soumi De (Syracuse), Christian Drischler, Madappa Prakash & Tianqi Zhao (Ohio), Sophia Han (TDLI), Evgeni Kolomeitsev (Matej Bei, Slovakia), Akira Ohnishi (YITP, Kyoto), Sanjay Reddy (INT), Achim Schwenk (Darmstadt), Andrew Steiner (Tennessee) & Ingo Tews (LANL)

Nuclear Symmetry Energy and Pressure

The symmetry energy is the difference between the energies of pure neutron matter ($x = 0$) and symmetric ($x = 1/2$) nuclear matter:

$$S(n) = E(n, x = 0) - E(n, x = 1/2).$$

The quadratic term in an expansion of neutron excess $1 - 2x$ dominates:

$$E(n, x) = E(n, 1/2) + (1-2x)^2 S_2(n) + \ldots$$

Expanding S_2 about saturation n_s:

$$S_2(n) = \mathbf{J} + \frac{\mathbf{L}}{3}\frac{n - n_s}{n_s} + \ldots$$

$$\mathbf{J} \simeq 31 \text{ MeV}, \quad \mathbf{L} \simeq 50 \text{ MeV}$$

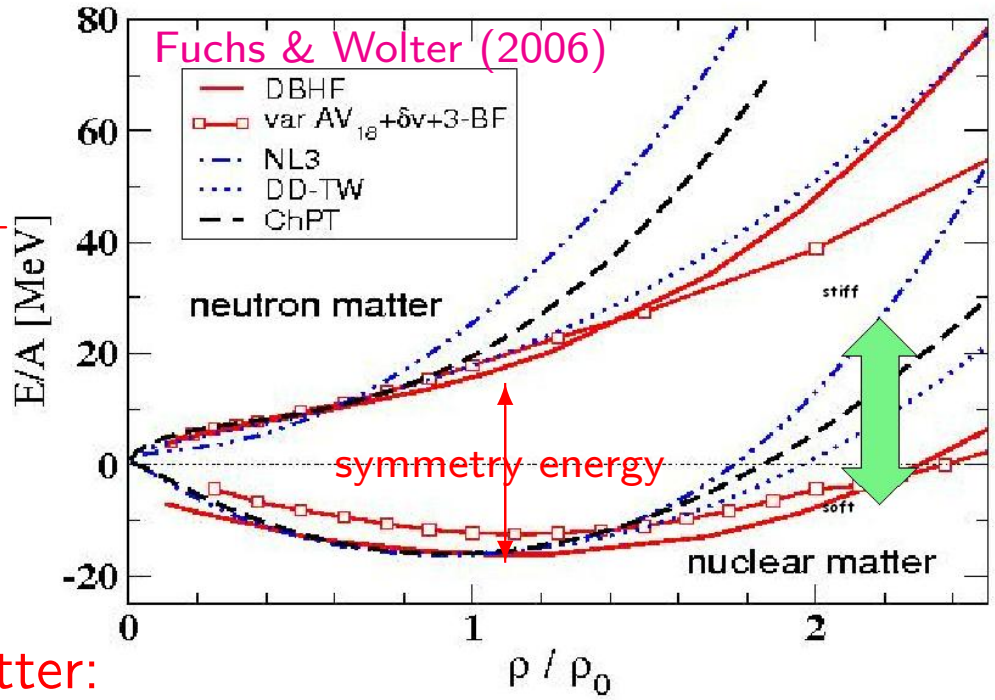

Extrapolated to pure neutron matter:

$$E_N = E(n_s, 0) \approx J + E(n_s, 1/2) \equiv J - B, \qquad P_N = P(n_s, 0) = L n_s/3$$

Neutron star matter (beta equilibrium) is nearly neutron matter:

$$\frac{\partial(E + E_e)}{\partial x} = 0, \quad P_{NSM}(n_s) \simeq \frac{L n_s}{3}\left[1 - \left(\frac{4J}{\hbar c}\right)^3 \frac{4 - 3J/L}{3\pi^2 n_s}\right]$$

Why is the Symmetry Energy Important?

The equation of state in a neutron star depends strongly on the density dependance of the symmetry energy ($u = n_B/n_s$):

$$P_{NSM}(u) \simeq n_s u^2 \left[\frac{L}{3} + \frac{K_N}{9}(u-1) + \frac{Q_N}{54}(u-1)^2 + \cdots \right].$$

A strong correlation exists between radii and P_{NSM} near n_s: $R_{1.4} \sim P_{NSM}(n_B)^{1/4}$.

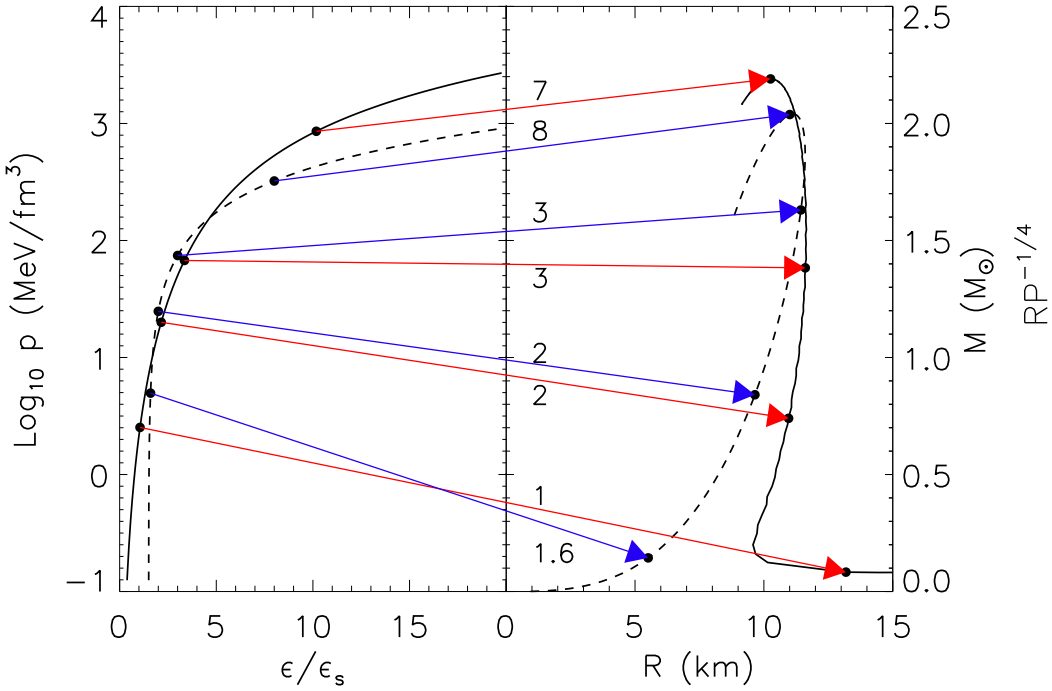

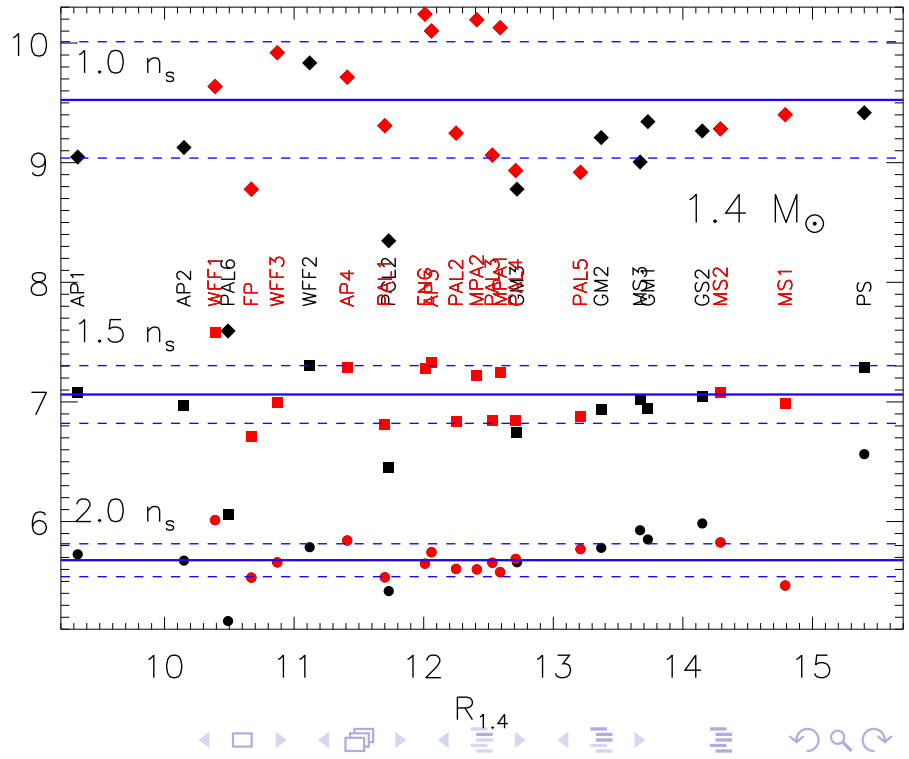

Symmetry Parameter Correlation from Masses

Liquid drop model approximately valid

$$E_{\rm sym}(N,Z) = (JA - S_s A^{2/3}) I^2$$

$$\chi^2 = \frac{1}{\mathcal{N}\sigma_D^2}\sum_{i=1}^{\mathcal{N}}(E_{ex,i} - E_{sym,i})^2$$

$$\chi_{JJ} = \frac{2}{\mathcal{N}\sigma_D^2}\sum_{i=1}^{\mathcal{N}} I_i^4 A_i^2 \simeq 61.6\,\sigma_D^{-2}$$

$$\chi_{ss} = \frac{2}{\mathcal{N}\sigma_D^2}\sum_{i=1}^{\mathcal{N}} I_i^4 A_i^{4/3} \simeq 1.87\,\sigma_D^{-2}$$

$$\chi_{Js} = -\frac{2}{\mathcal{N}\sigma_D^2}\sum_{i=1}^{\mathcal{N}} I_i^4 A_i^{5/3} \simeq -10.7\,\sigma_D^{-2}$$

$$\sigma_J = \sqrt{\frac{2\chi_{ss}}{\chi_{JJ}\chi_{ss} - \chi_{Js}^2}} \simeq 2.3\,\sigma_D$$

$$\sigma_{S_s} = \sqrt{\frac{2\chi_{JJ}}{\chi_{JJ}\chi_{ss} - \chi_{Js}^2}} \simeq 13.2\,\sigma_D$$

$$\alpha = \frac{1}{2}\tan^{-1}\frac{2\chi_{Js}}{\chi_{JJ} - \chi_{ss}} \simeq 9^\circ.8$$

$$r_{Js} = -\frac{\chi_{Js}}{\sqrt{\chi_{JJ}\chi_{ss}}} \simeq 0.997$$

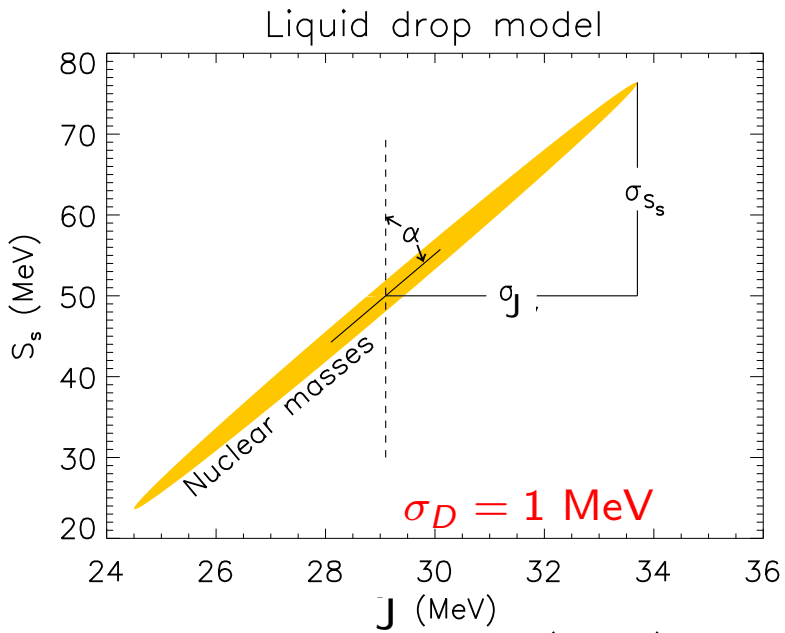

Kortelainen et al. (2010)

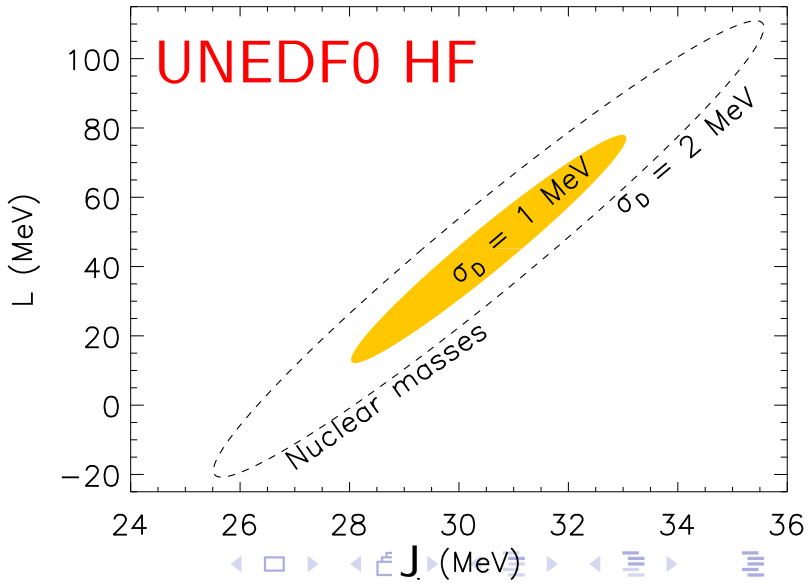

Determining S_S

S_S is non-zero because $S(u)$ decreases from the center to the surface. Minimization of the total nuclear energy leads to

$$\frac{S_S}{J} = \frac{E_s}{2} \frac{\int_0^1 u^{1/2}[J/S(u) - 1][E(u, 1/2) + B]^{-1/2} du}{\int_0^1 [E(u, 1/2) + B]^{1/2} du},$$

$E_s \simeq 18$ MeV is the symmetric matter surface energy coefficient in the liquid droplet mass formula.

The relation is nearly perfectly linear, $S_S/J = (0.764 \pm 0.130) + 0.0234L$.

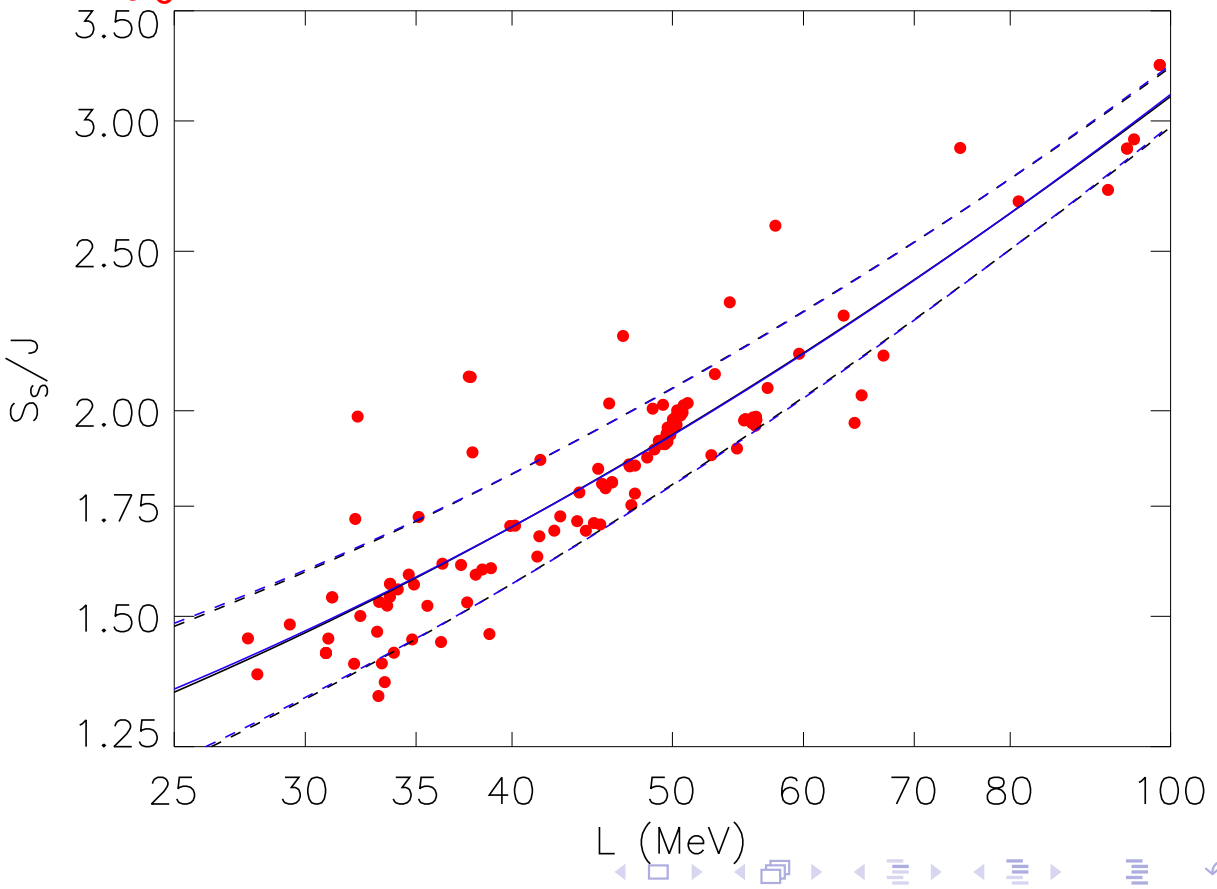

Fitting Nuclear Binding Energies

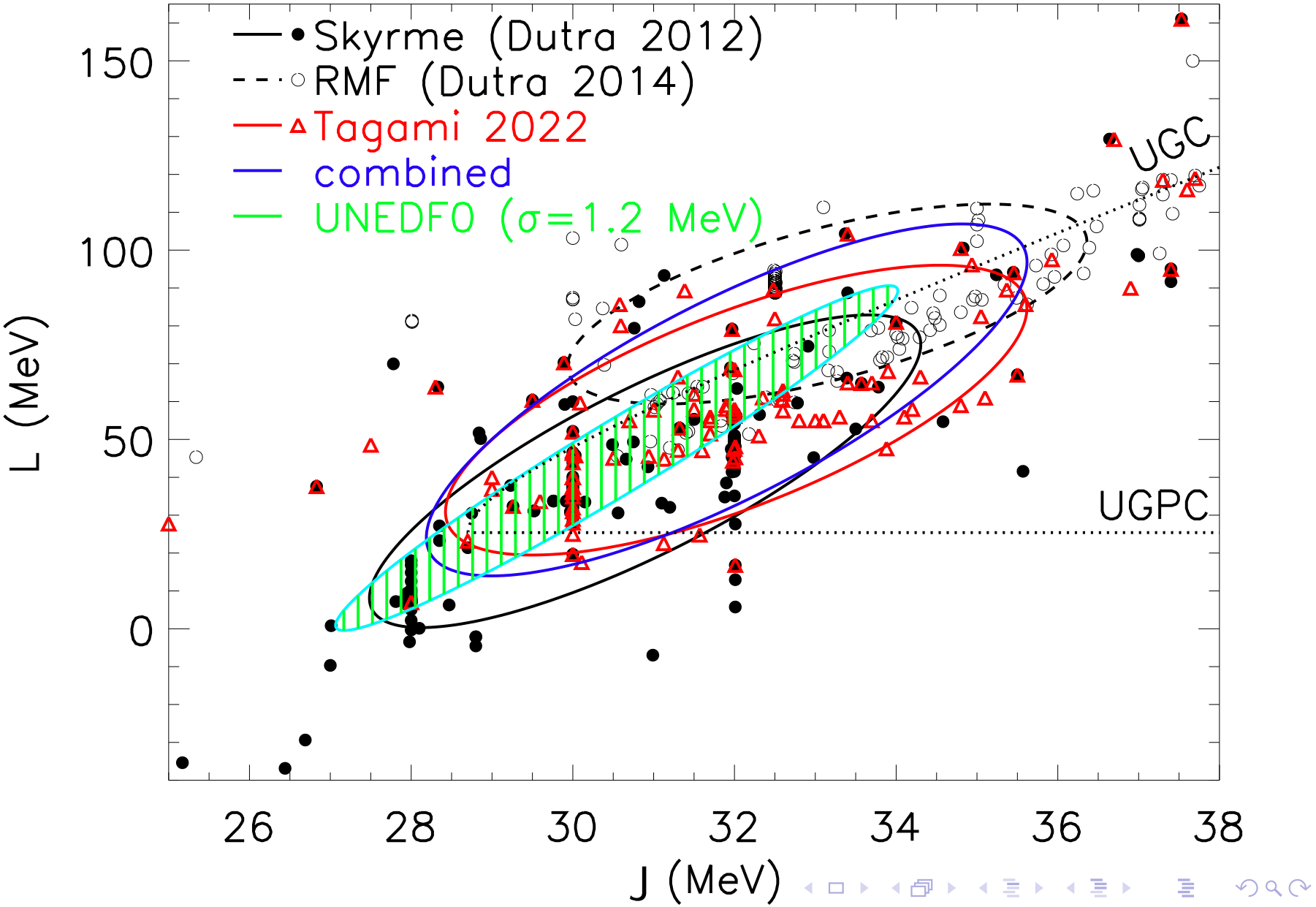

Meaning of $J - L$ Correlation

The slope dL/dJ is an indicator of the most sensitive density u_s for the measurement of the symmetry energy $S(u)$.

If the correlation line goes through (J, L), a change dJ can be compensated by a change dL.

$$\frac{dJ}{dL} = -\left(\frac{\partial S(u_s)}{\partial L}\right)_J \Bigg/ \left(\frac{\partial S(u_s)}{\partial J}\right)_L .$$

Example: $S(u) = S_K u^{2/3} + S_V u^\gamma, \quad S_K \simeq 12.5 \text{ MeV}$
$J = S_K + S_V, \quad L = 2S_K + 3\gamma S_V = S_K(2 - 3\gamma) + 3\gamma J$

$$\frac{dJ}{dL} = -\frac{\ln u_s}{3}, \quad u_s = \exp\left(-3\frac{dJ}{dL}\right).$$

For binding energies, $dL/dJ \simeq 11, \quad u_s \simeq 0.76.$

Saturation Properties of Nuclear Interactions

Empirical Saturation Window

$B = 16.06 \pm 0.20$ MeV

$n_s = 0.1558 \pm 0.0054$ fm^{-3}

$K_{1/2} = 236.5 \pm 15.4$ MeV

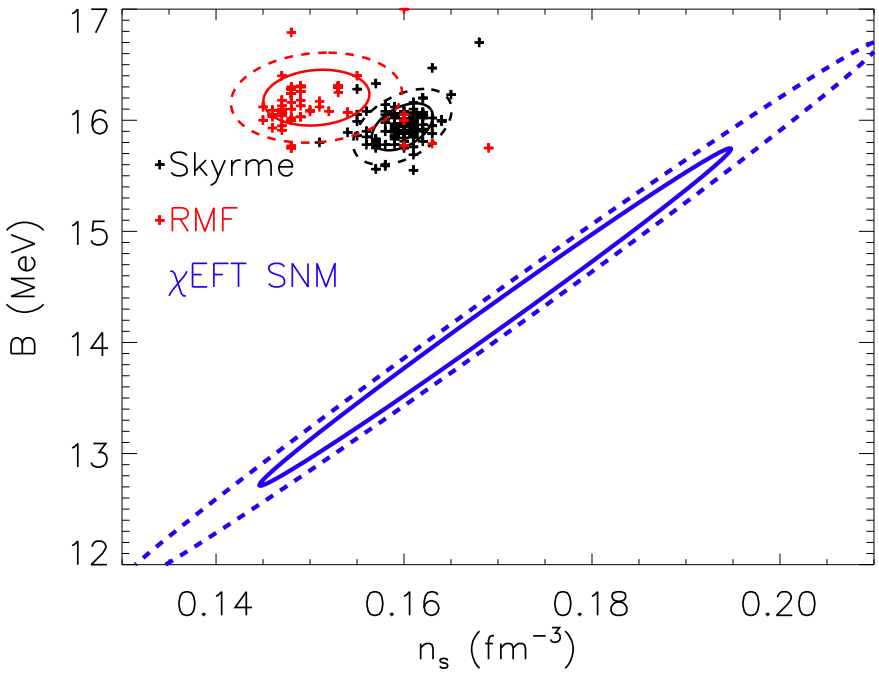

Data from Dutra (2012, 2014)

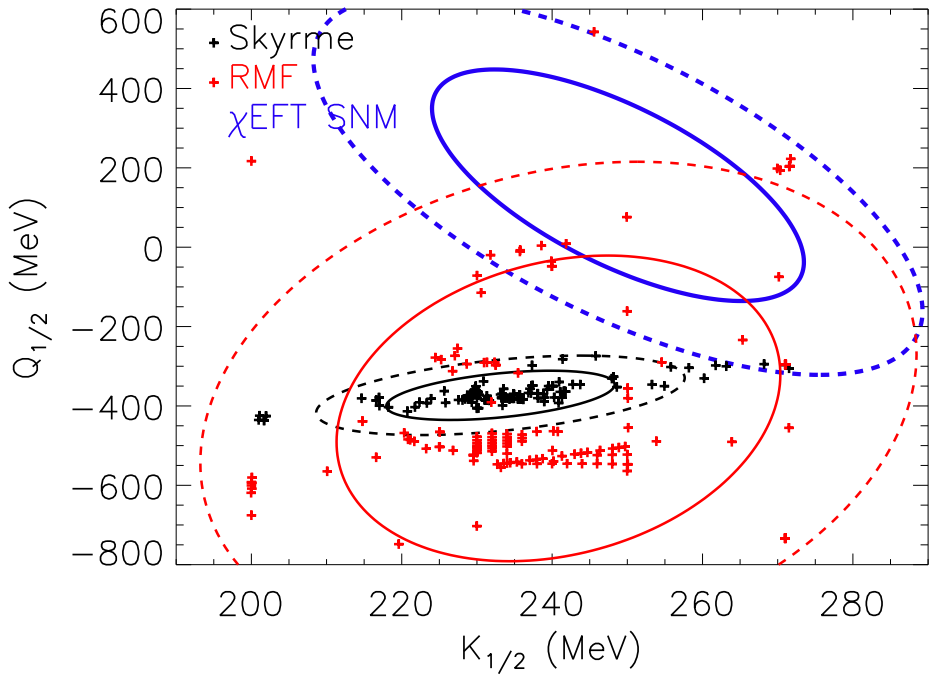

Theoretical Neutron Matter Studies

Recently developed chiral effective field theory allows a systematic expansion of nuclear forces at low energies based on the symmetries of quantum chromodynamics. It exploits the gap between the pion mass (the pseudo-Goldstone boson of chiral symmetry-breaking) and the energy scale of short-range nuclear interactions established from experimental phase shifts. It provides the only known consistent framework for estimating energy uncertainties.

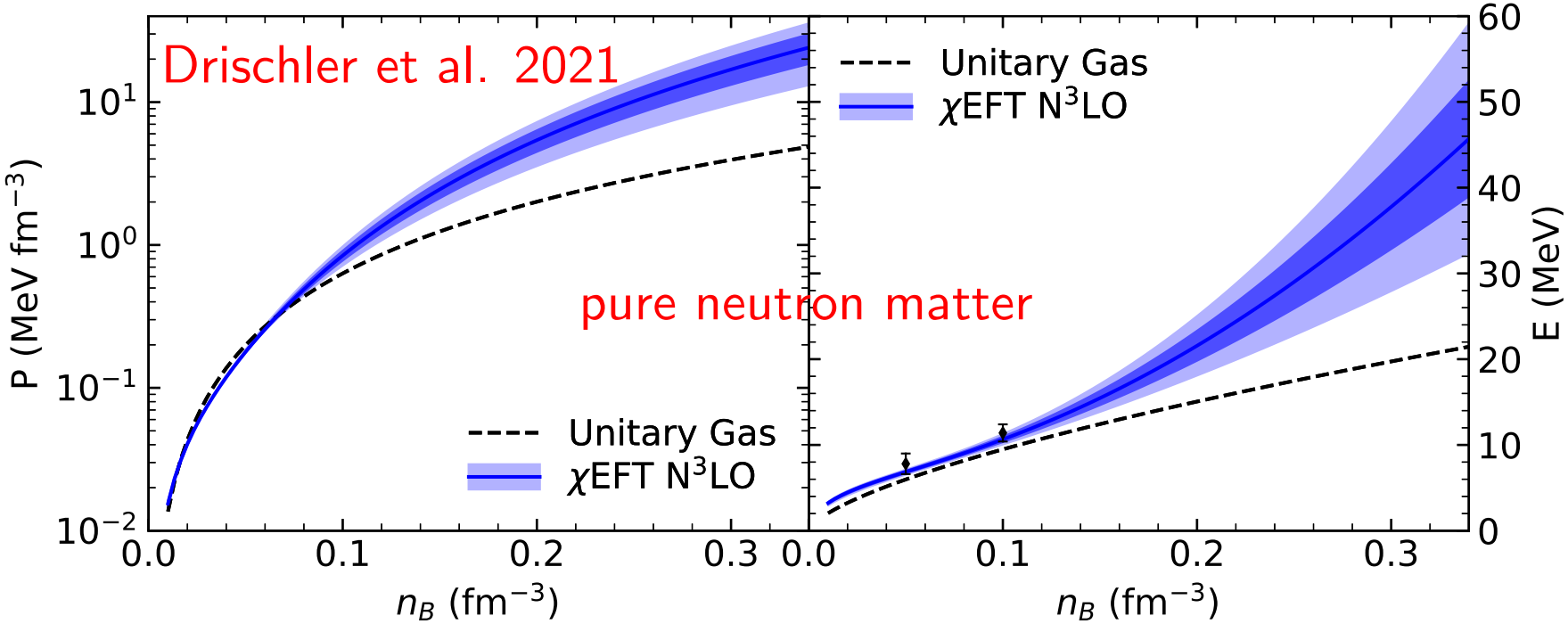

Symmetry Parameters From Chiral EFT

Two approaches to extracting J and L

1. Take the difference between pure neutron and symmetric matter energies and pressures at the calculated saturation density.

2. Use pure neutron matter energy and pressure with the empirical saturation window from nuclear mass fits.

$J = E_N(n_s) + B,$

$L = 3P_N(n_s)/n_s.$

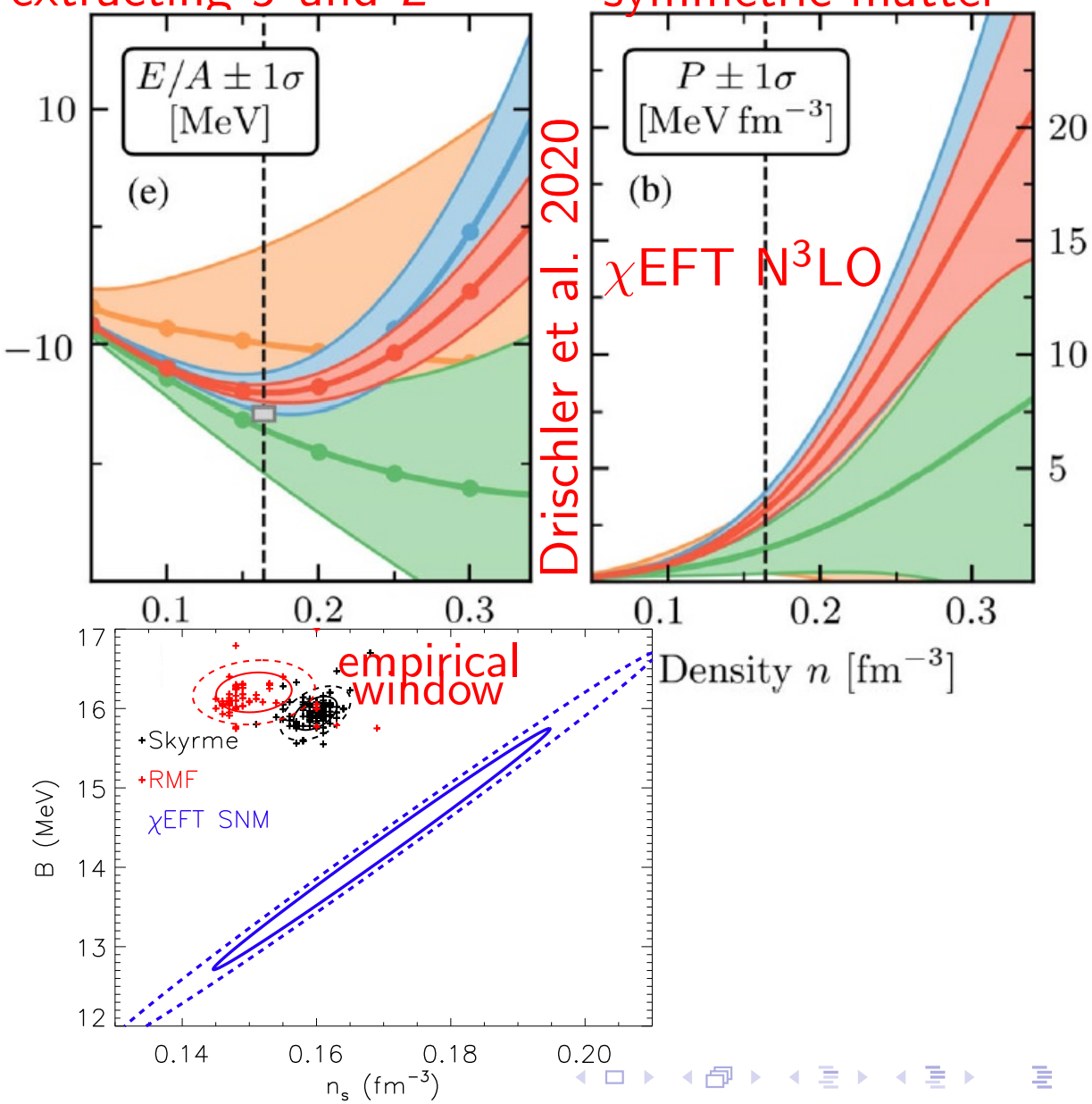

Symmetry Parameters From Neutron Matter

Pure neutron matter calculations are more reliable than symmetric matter calculations.

Symmetric matter emerges from a delicate cancellation sensitive to short- and intermediate-range three-body interactions at N^2LO that are Pauli-blocked in pure neutron matter.

N^3LO symmetric matter calculations don't saturate within empirical ranges for n_s and B, and introduce spurious correlations in symmetric matter.

We infer symmetry parameters from $E_N(n_s)$ and $P_N(n_s)$ using

$$J = E_N(n_s) + B$$

$$L = 3P_N(n_s)/n_s$$

and include uncertainties in E_N, P_N, n_s and B.

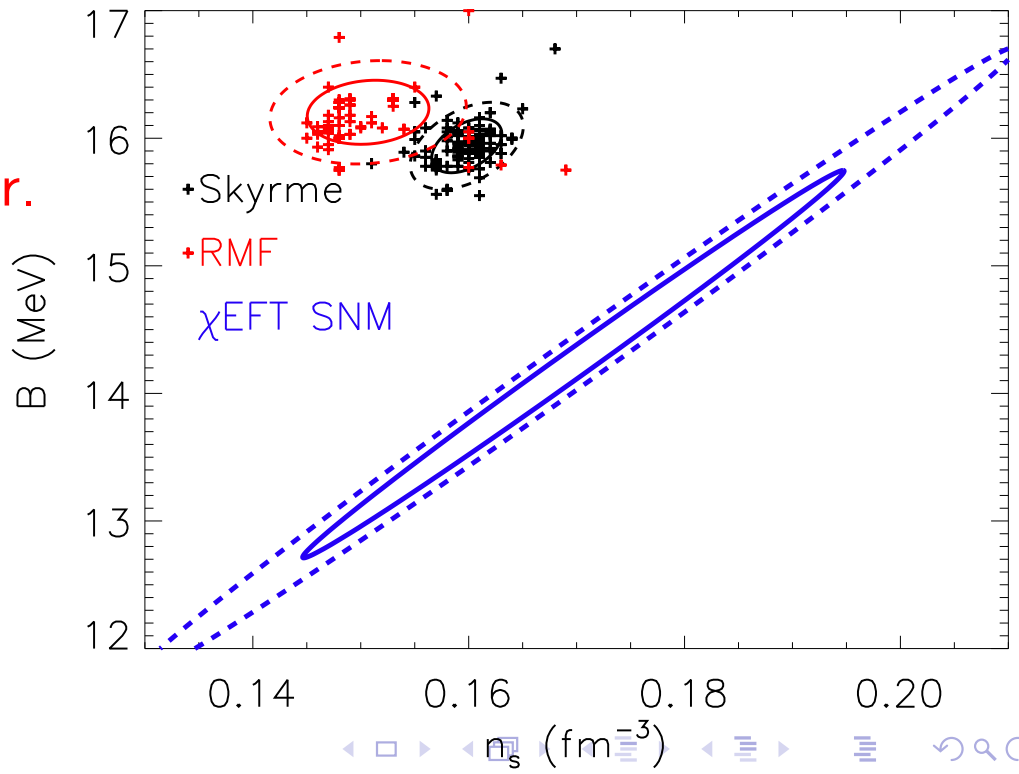

Correlations From Chiral EFT

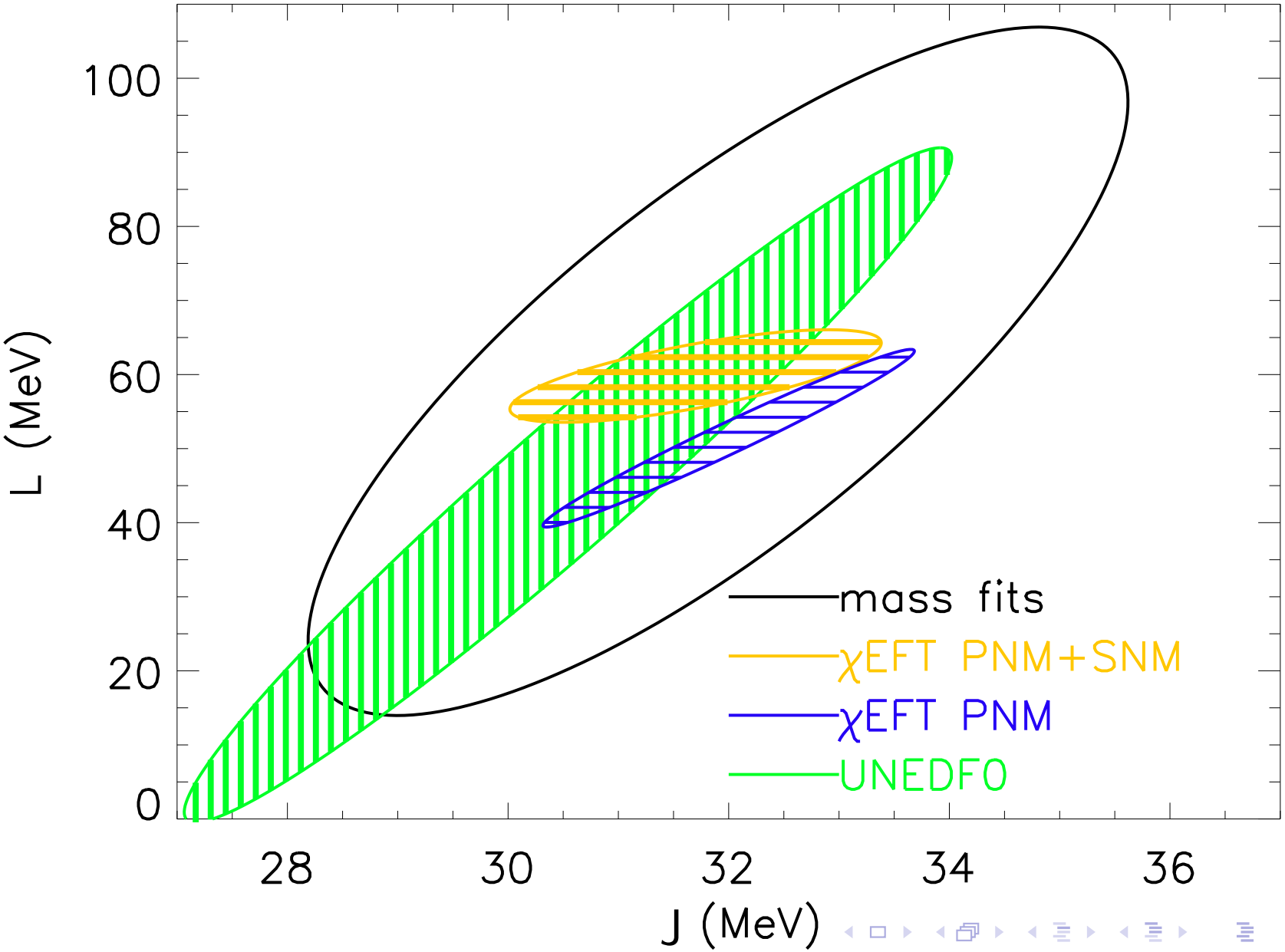

Bounds From The Unitary Gas Conjecture

The Conjecture (UGC):

Neutron matter energy always larger than unitary gas energy.

$E_{UG} = \xi_0 (3/5) E_F$, or

$$E_{UG} \simeq 12.6 \left(\frac{n}{n_s} \right)^{2/3} \text{MeV}.$$

The unitary gas consists of fermions interacting via a pairwise short-range s-wave interaction with infinite scattering length and zero range. Cold atom experiments show a universal behavior with the Bertsch parameter $\xi_0 \simeq 0.37$.

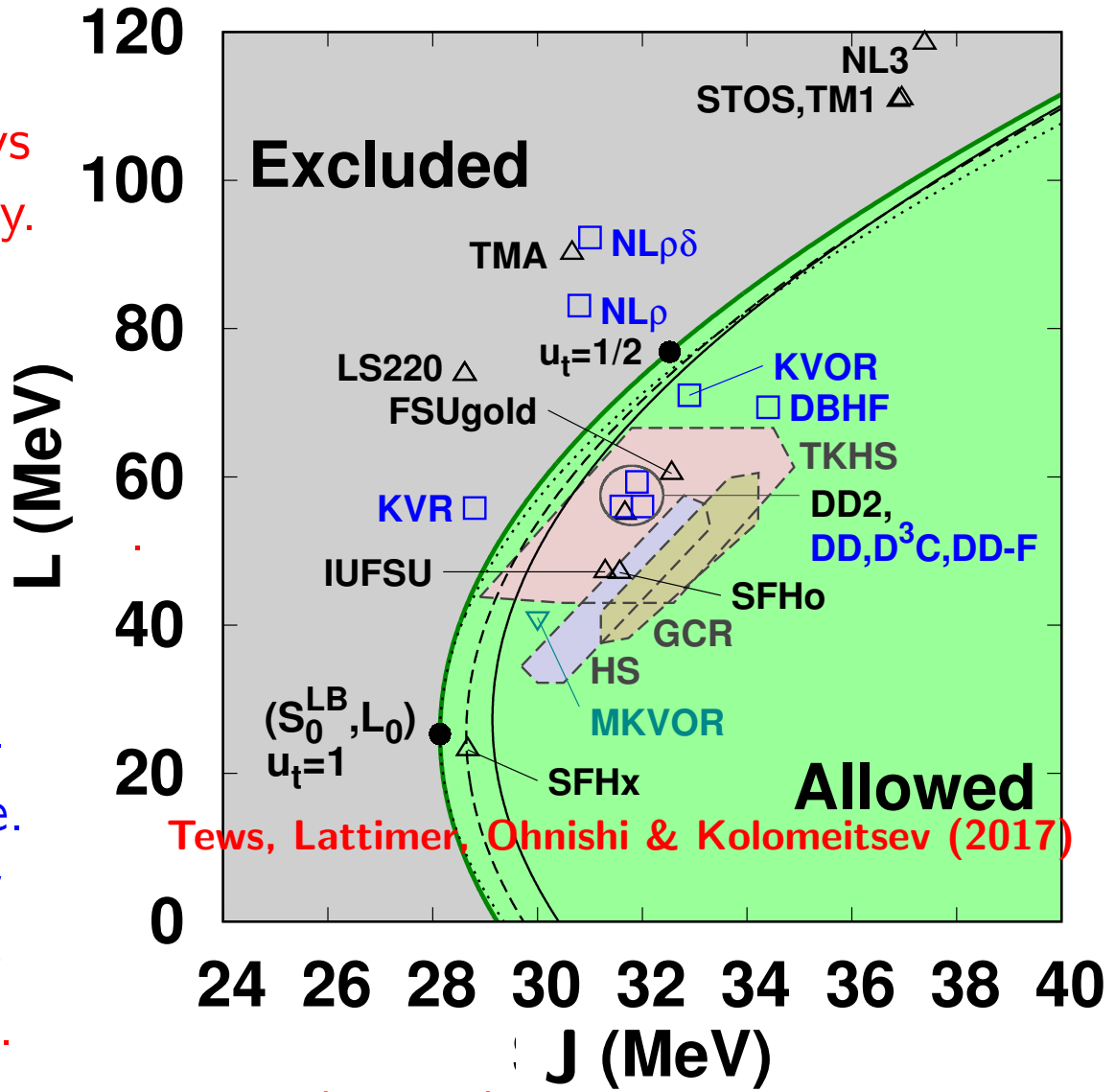

For $n \geq n_s$, one also observes $P_N > P_{UG}$ (UGPC).

$J \geq 28.6$ MeV; $L \geq 25.3$ MeV; $P_N(n_s) \geq 1.35$ MeV fm^{-3}; $R_{1.4} \geq 9.7$ km

Applying Unitary Gas Constraints

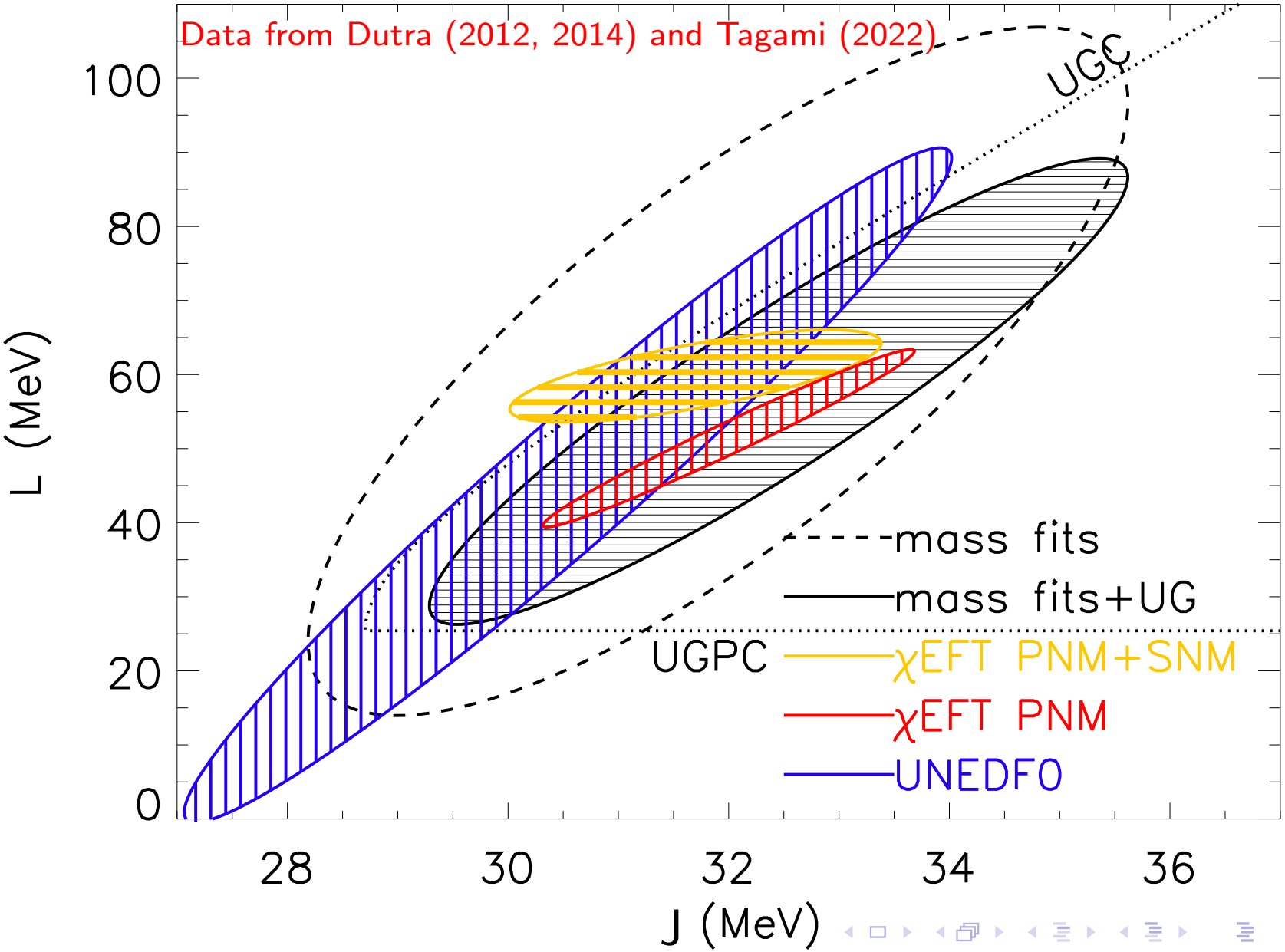

$K_N - L$ Correlations

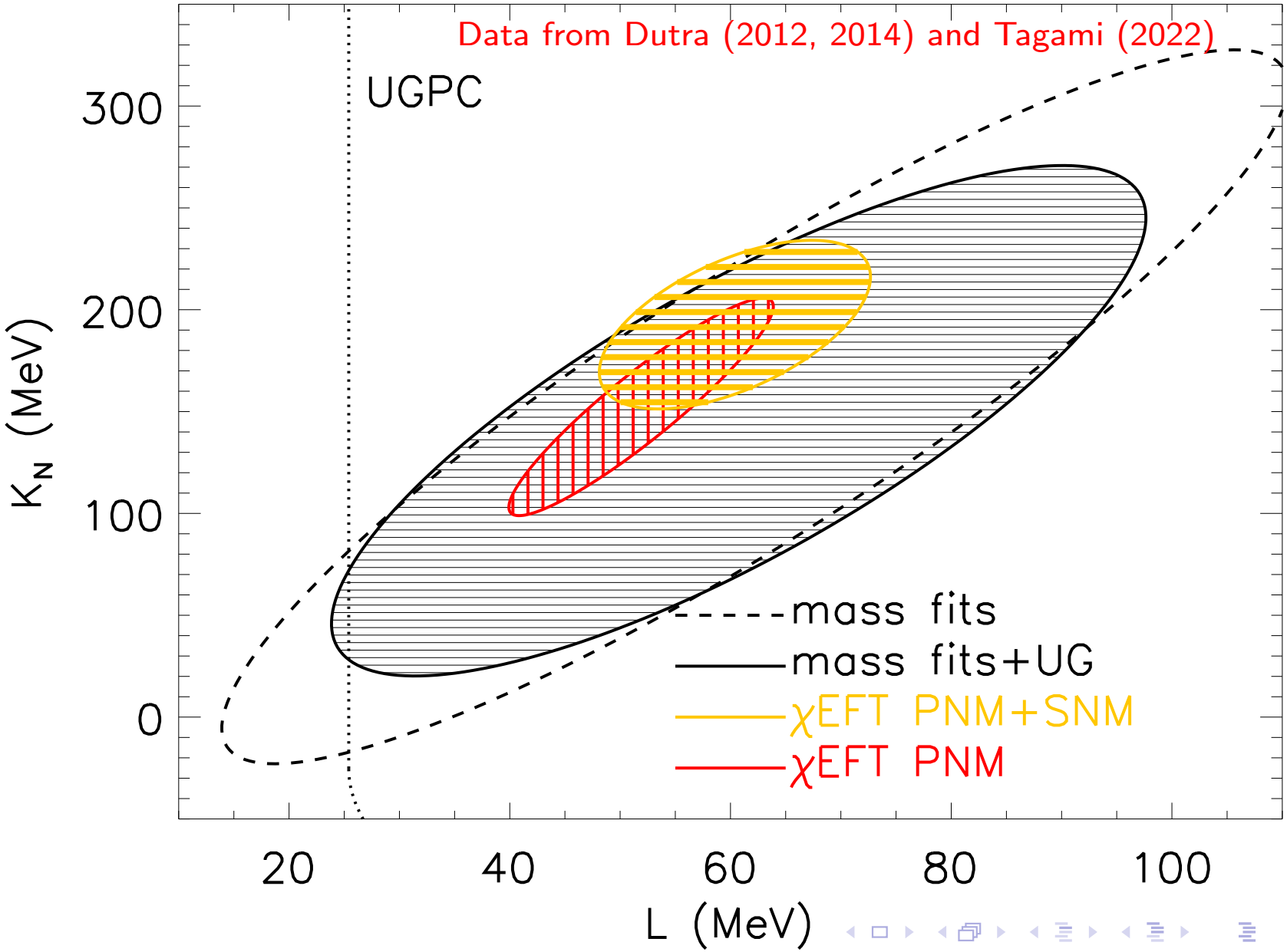

Neutron Skin Thickness

The difference between the mean neutron and proton radii in the liquid droplet model is

$t_{np} = R_n - R_p$.

The mean square difference is

$r_{np}^2 = < R_n >^2 - < R_p >^2$.

$$r_{np} = \sqrt{\frac{3}{5}} \frac{2 r_o I}{3} \frac{S_s}{J} \left[1 + S_s A^{-1/3} / J \right]^{-1} f_C$$

Implies strong $L - r_{np}$ correlation.

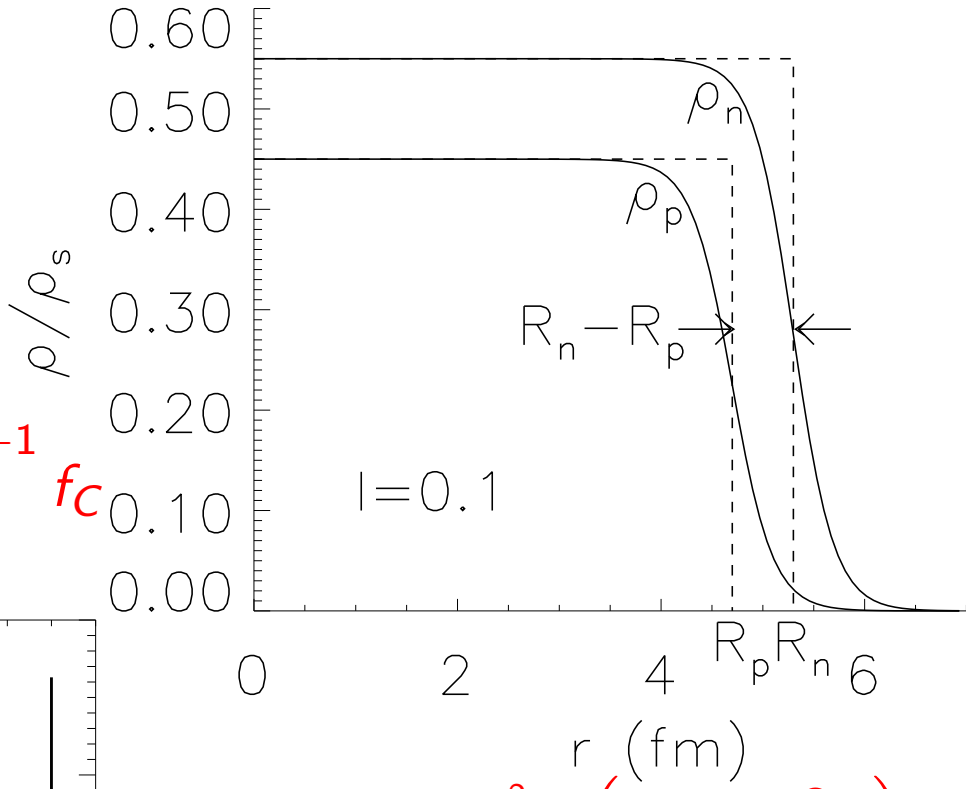

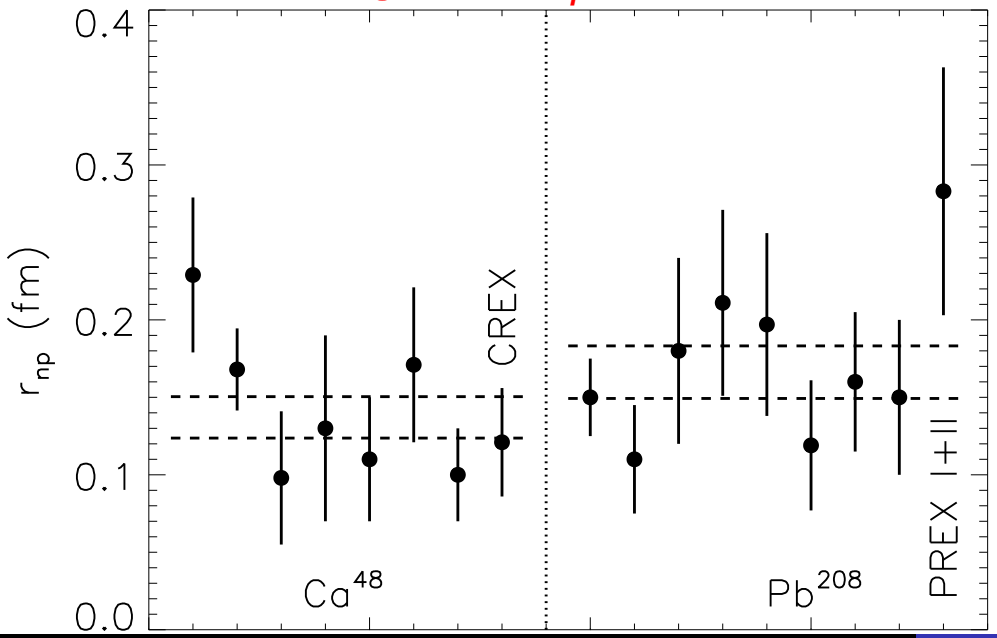

$$f_C = 1 - \frac{3Ze^2}{140 I S_S r_o} \left(1 + \frac{10 S_S}{3 J A^{1/3}} \right)$$

$$\frac{\Delta S_S / J}{\Delta J} \simeq -0.032$$

$$\frac{\Delta L}{\Delta J} = \frac{\Delta S_S / J}{\Delta J} \frac{1}{0.0234} \simeq -1.4$$

Calculated $L - r_{np}$ Correlations

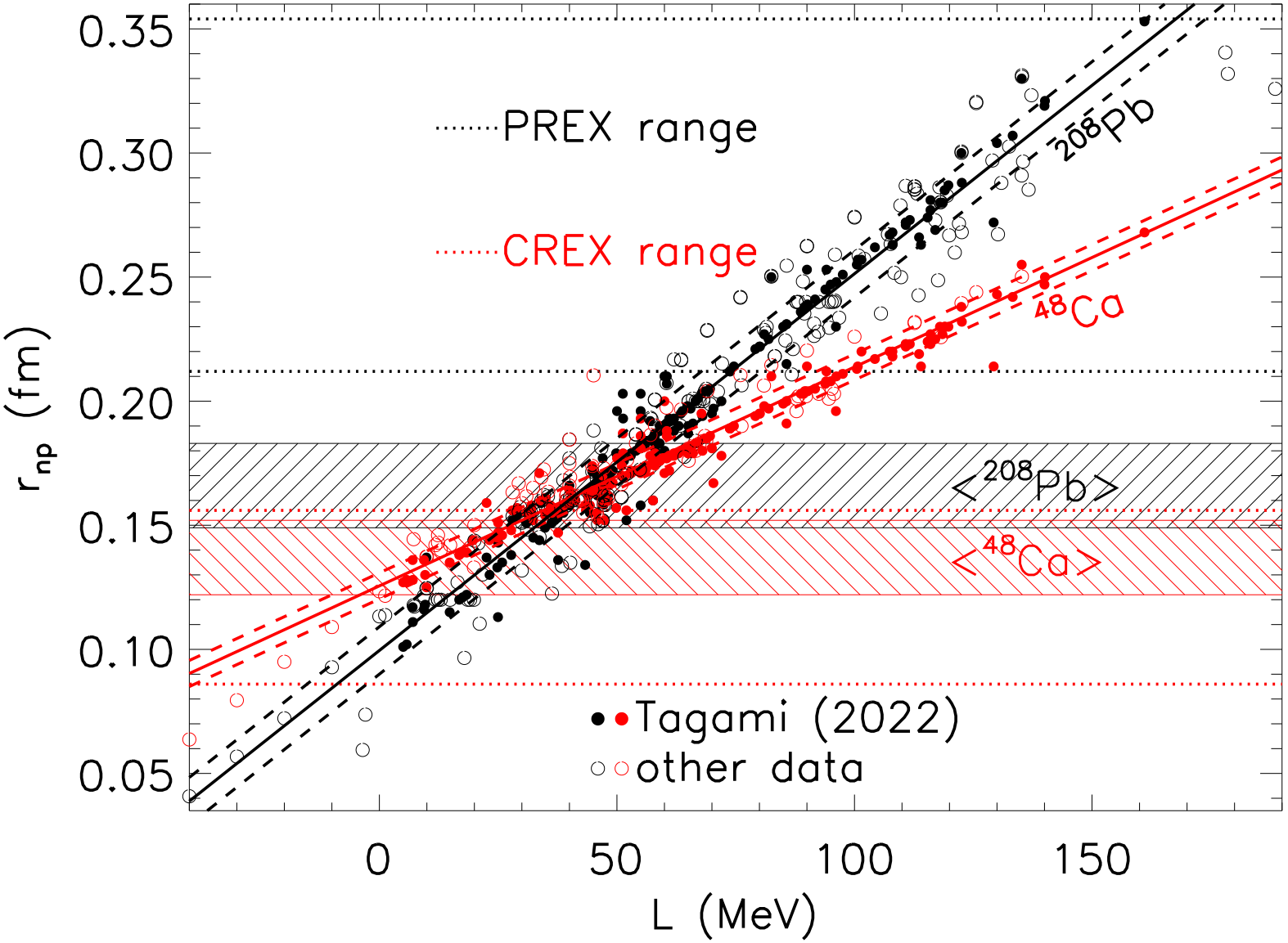

Implied L Values

Historical experimental weighted average ^{208}Pb
$r_{np}^{208} = 0.166 \pm 0.017$ fm, implying $L = 45 \pm 13$ MeV.

Historical experimental weighted average ^{48}Ca
$r_{np}^{48} = 0.137 \pm 0.015$ fm, implying $L = 14 \pm 21$ MeV.

Combined $L = 36 \pm 11$ MeV.

Parity-violating electron scattering measurements at JLab:

PREX I+II ^{208}Pb (Adhikari et al. 2021):
$r_{np}^{208} = 0.283 \pm 0.071$ fm, implying $L = 119 \pm 46$ MeV.

CREX ^{48}Ca (Adhikari et al. 2022):
$r_{np}^{48} = 0.121 \pm 0.035$ fm, implying $L = -5 \pm 42$ MeV.

Combined $L = 51 \pm 31$ MeV.

$r_{np}^{208} - r_{np}^{48}$ Linear Correlation

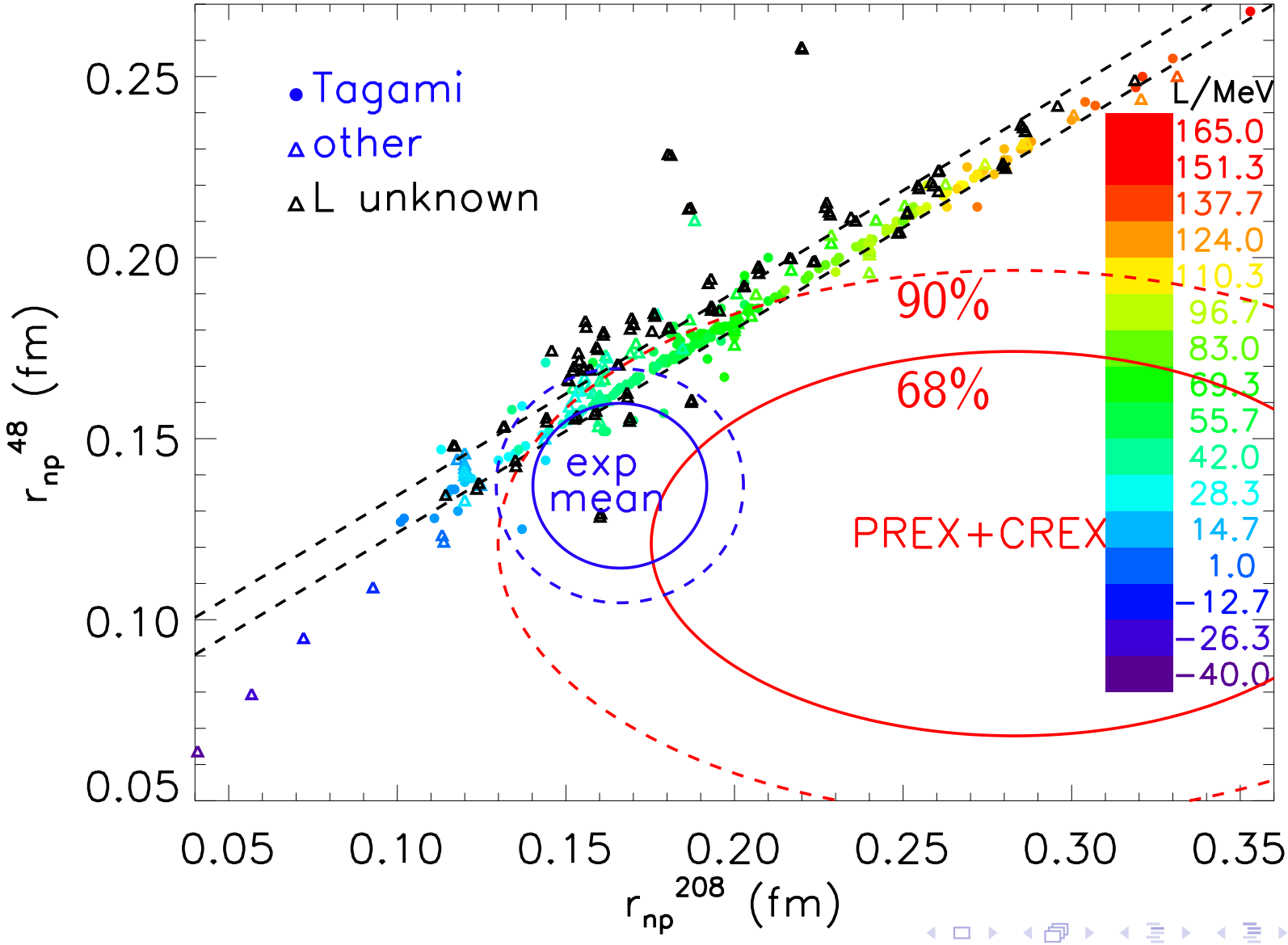

Detail

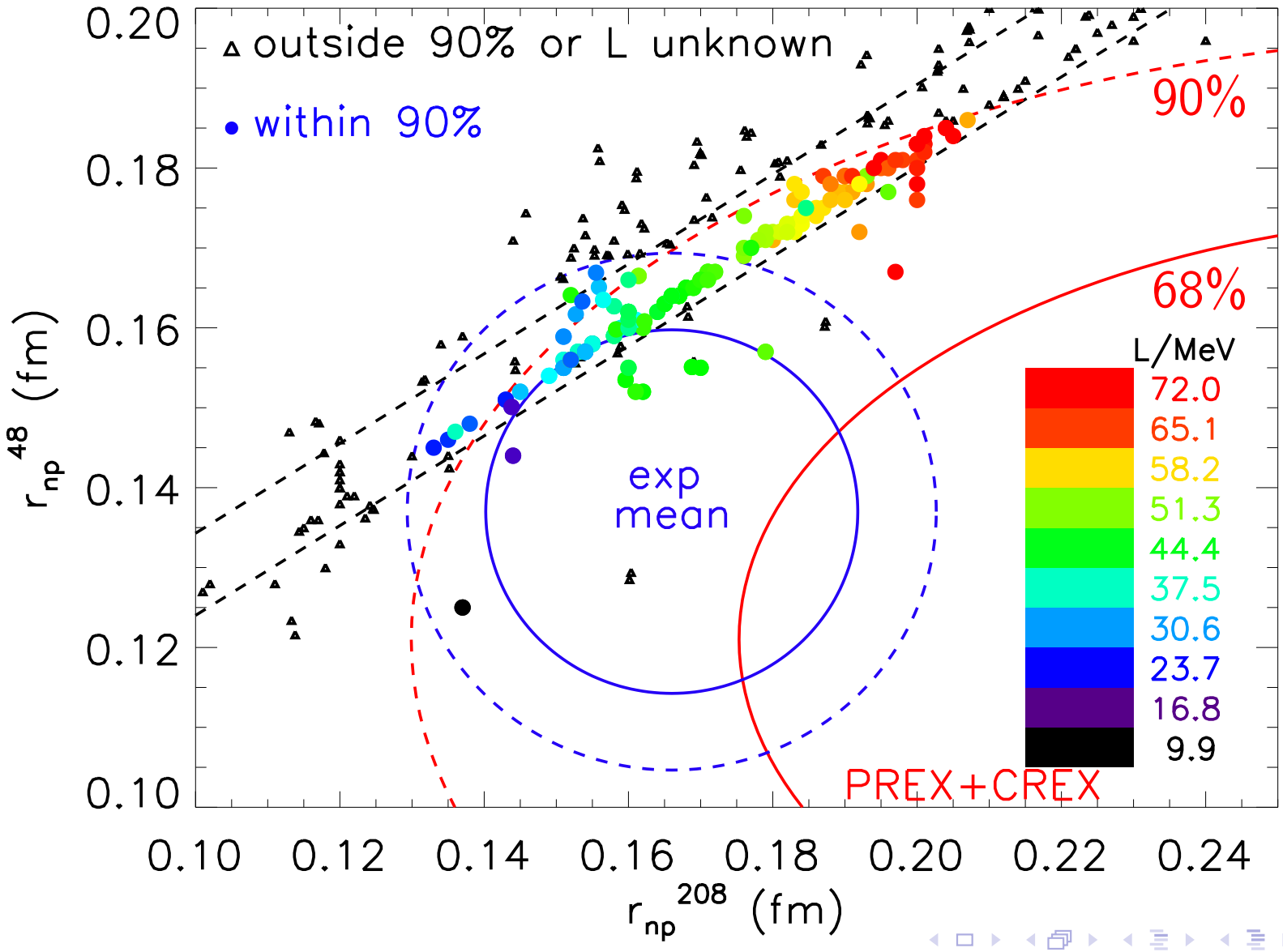
outside 90% or L unknown
within 90%
90%
68%
exp
mean
PREX+CREX
L/MeV
72.0
65.1
58.2
51.3
44.4
37.5
30.6
23.7
16.8
9.9
0.20
0.18
0.16
0.14
0.12
0.10
0.10
0.12
0.14
0.16
0.18
0.20
0.22
0.24
r_{np}^{48} (fm)
r_{np}^{208} (fm)

Implied $J - L$

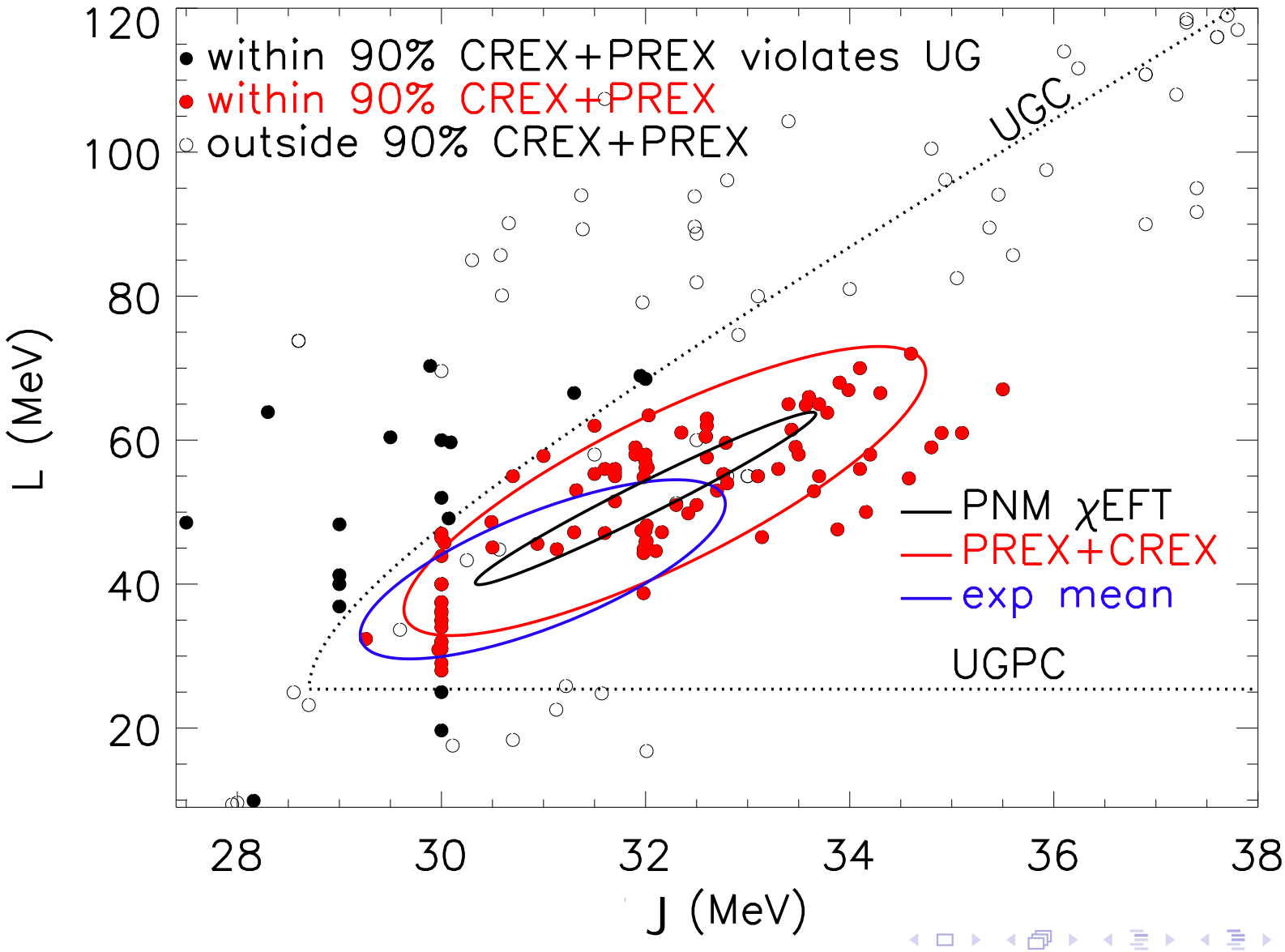
within 90% CREX+PREX violates UG
within 90% CREX+PREX
outside 90% CREX+PREX
UGC
PNM χEFT
PREX+CREX
exp mean
UGPC
L (MeV)
J (MeV)
120
100
80
60
40
20
28
30
32
34
36
38

Implied $K_N - L$

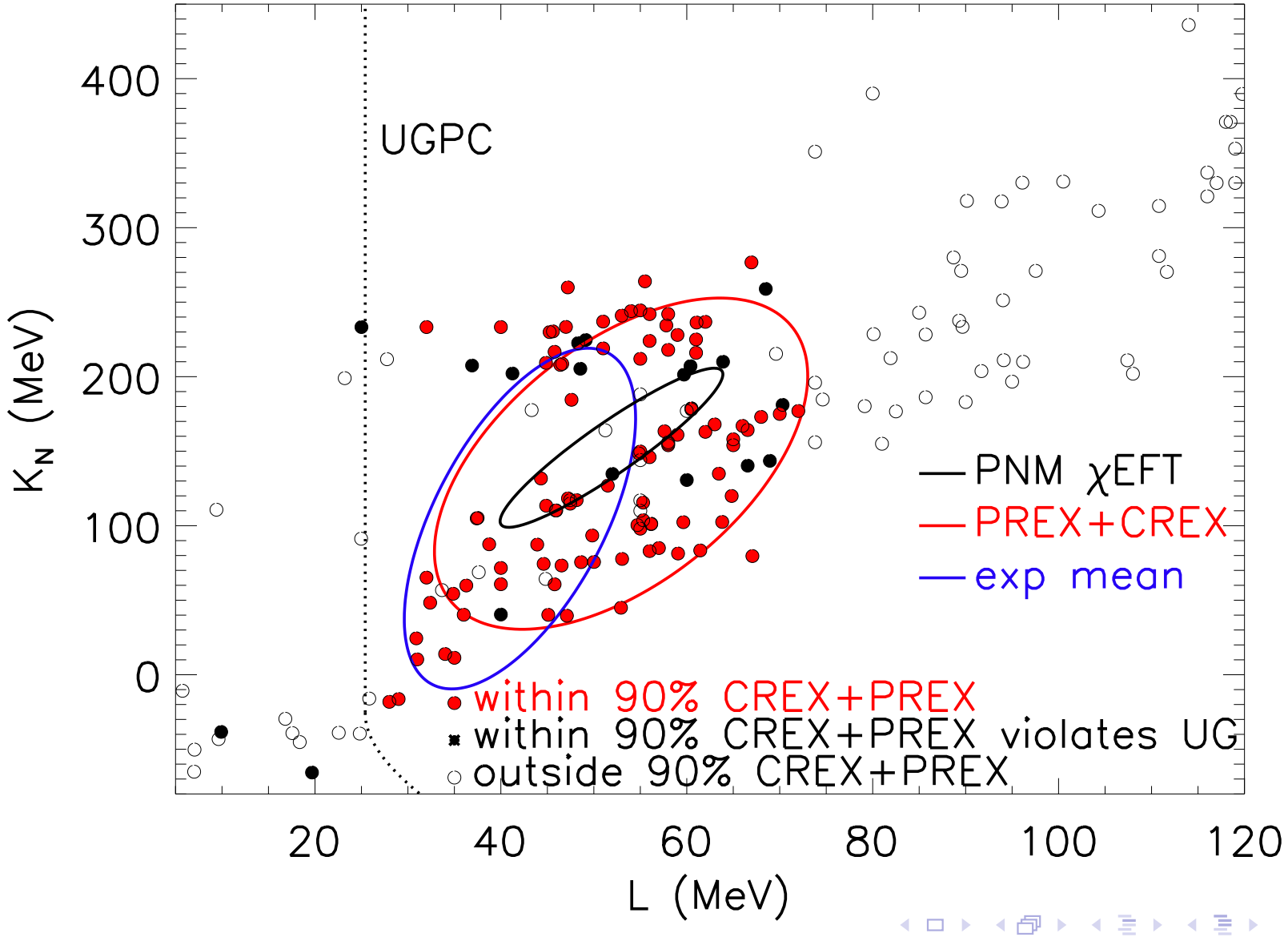
UGPC
PNM χEFT
PREX+CREX
exp mean
within 90% CREX+PREX
within 90% CREX+PREX violates UG
outside 90% CREX+PREX
K_N (MeV)
L (MeV)
400
300
200
100
0
20
40
60
80
100
120

Giant Dipole Resonances

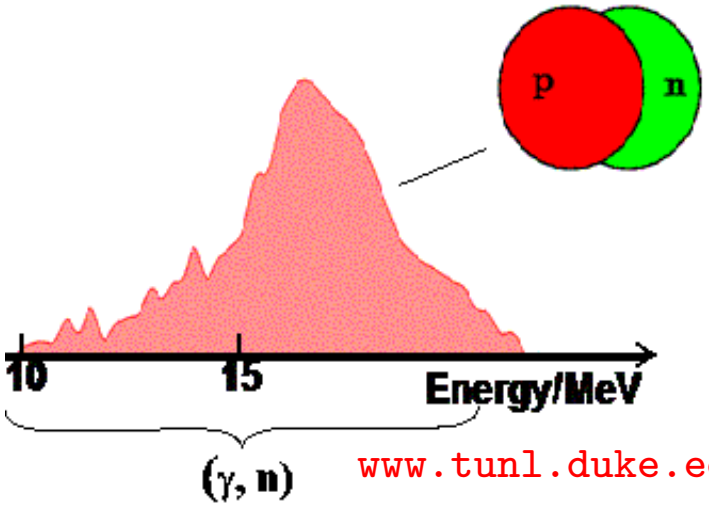

$$E_{-1} \propto J\left(J + \frac{5S_s}{3A^{1/3}}\right)^{-1/2}$$

$S(0.1\ \mathrm{fm}^{-3}) = 24.1 \pm 0.8$ MeV
Trippa et al. (2008)

$S(0.05\ \mathrm{fm}^{-3}) = 16.5 \pm 1.0$ MeV
Zhang et al. (2015)

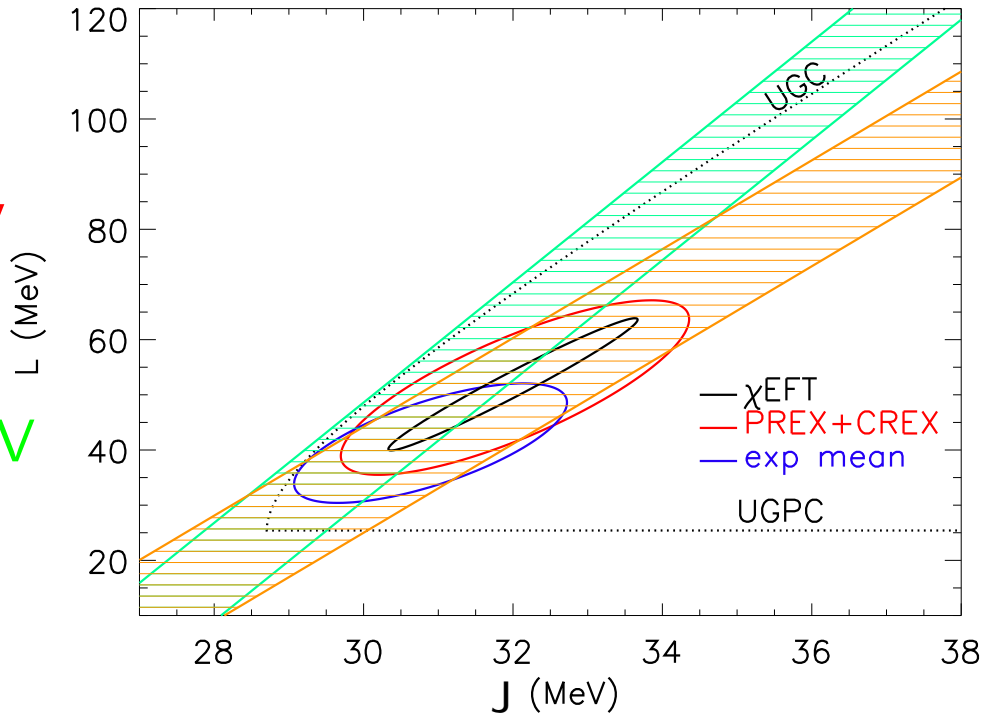

Dipole Polarizability

The linear response, or dynamic polarizability, of a nucleus excited from its ground state to an excited state due to an external oscillating dipolar field. In the liquid droplet model

$$\alpha_D J = \frac{AR^2}{20}\left(1 + \frac{5}{3}\frac{S_s}{J}A^{-1/3}\right)$$

Hashimoto (2015) Sn: $\alpha_D^{120} = (8.59 \pm 0.37)\ \mathrm{fm}^3$
Tamii (2012) Pb: $\alpha_D^{208} = (19.6 \pm 0.6)\ \mathrm{fm}^3$
Birkhan (2017) Ca: $\alpha_D^{48} = (2.07 \pm 0.22)\ \mathrm{fm}^3$

Roca-Maza et al. (2015):

$$\begin{aligned} \alpha_D^{48} &= (0.10 \pm 0.01)\alpha_D^{208} + (0.36 \pm 0.07)\ \mathrm{fm}^3, \\ \alpha_D^{208} &= (2.2 \pm 0.1)\alpha_D^{120} + (0.1 \pm 0.5)\ \mathrm{fm}^3. \end{aligned}$$

Implies $\alpha_D^{48} = 2.32 \pm 0.21\ \mathrm{fm}^3$ and $\alpha_D^{208} = 19.0 \pm 1.2\ \mathrm{fm}^3$, consistent with measurements.

Dipole Polarizability Predictions for Skin Thickness

Roca-Maza et al. (2015), Piekarewicz (2021):

$$\begin{aligned}
\alpha_D^{48} J &= (355 \pm 44)\,(r_{np}^{48}/\mathrm{fm}) + (12 \pm 19)\ \mathrm{MeV\ fm^3}, \\
\alpha_D^{120} J &= (1234 \pm 93)\,(r_{np}^{120}/\mathrm{fm}) + (115 \pm 36)\ \mathrm{MeV\ fm^3}, \\
\alpha_D^{208} J &= (1922 \pm 73)\,(r_{np}^{208}/\mathrm{fm}) + (301 \pm 32)\ \mathrm{MeV\ fm^3},
\end{aligned}$$

Measured α_D^{48} and α_D^{208} and the average experimental value for r_{np}^{48} predict $r_{np}^{208} = (0.171 \pm 0.015)$ fm, almost exactly the average experimental value but significantly smaller than the PREX I+II measurement.

Conversely, the predicted value for r_{np}^{48} is constent with its average experimental value but slightly larger than the CREX measurement.

The Radius – Pressure Correlation

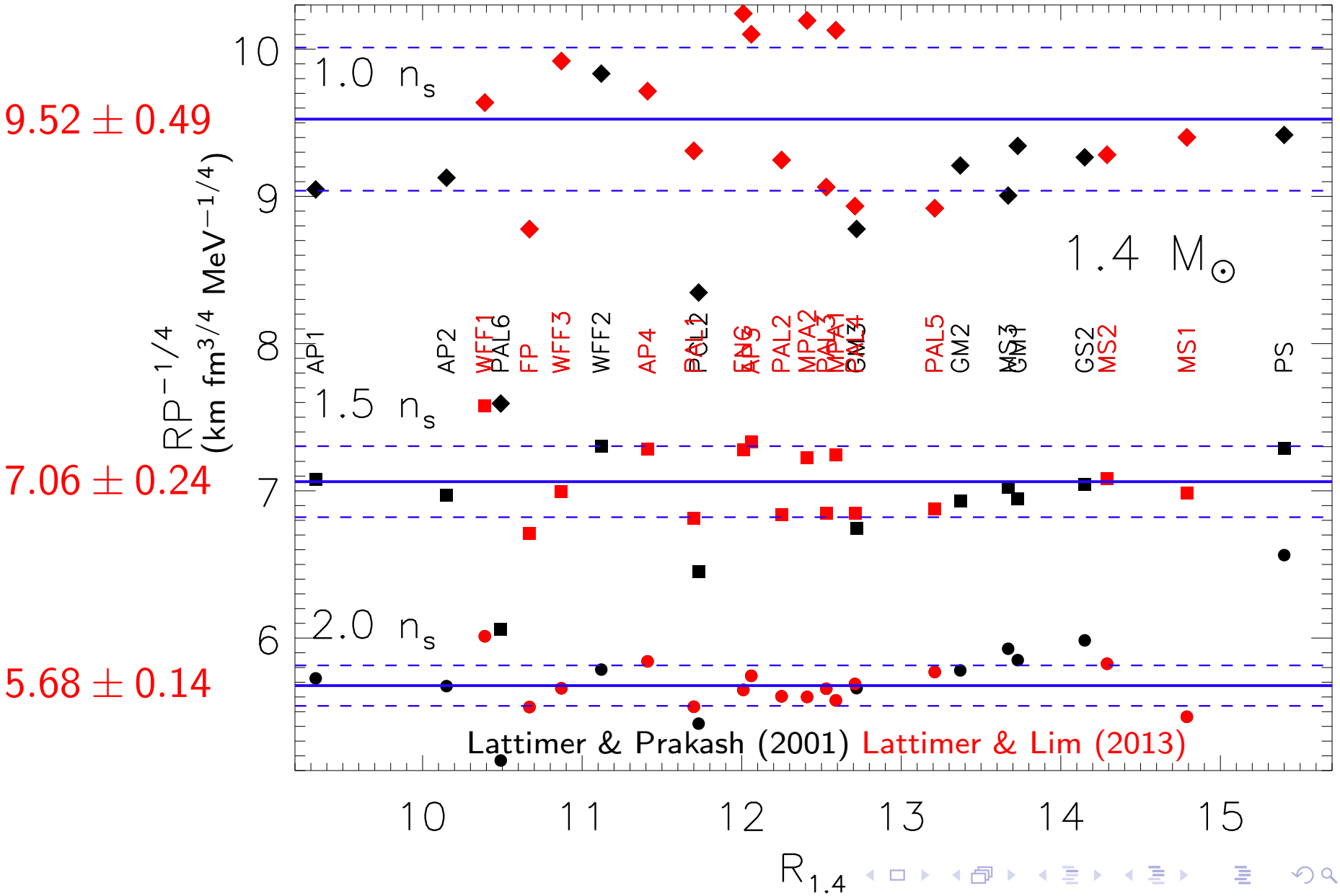

Implied $R_{1.4} - L$

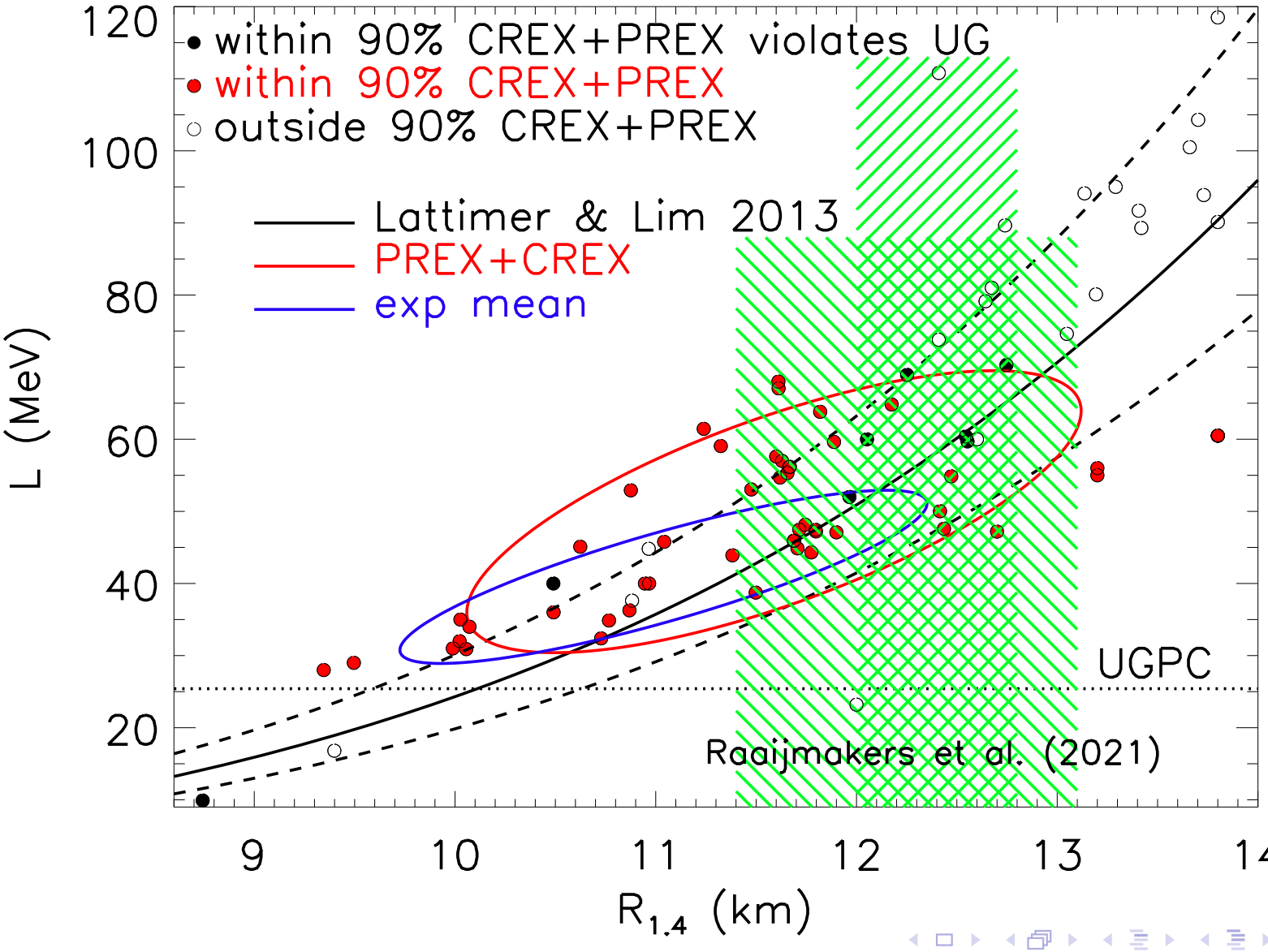

Neutron Star Interior Composition ExploreR (NICER)

Science Measurements

NICER

Reveal stellar structure through lightcurve modeling, long-term timing, and pulsation searches

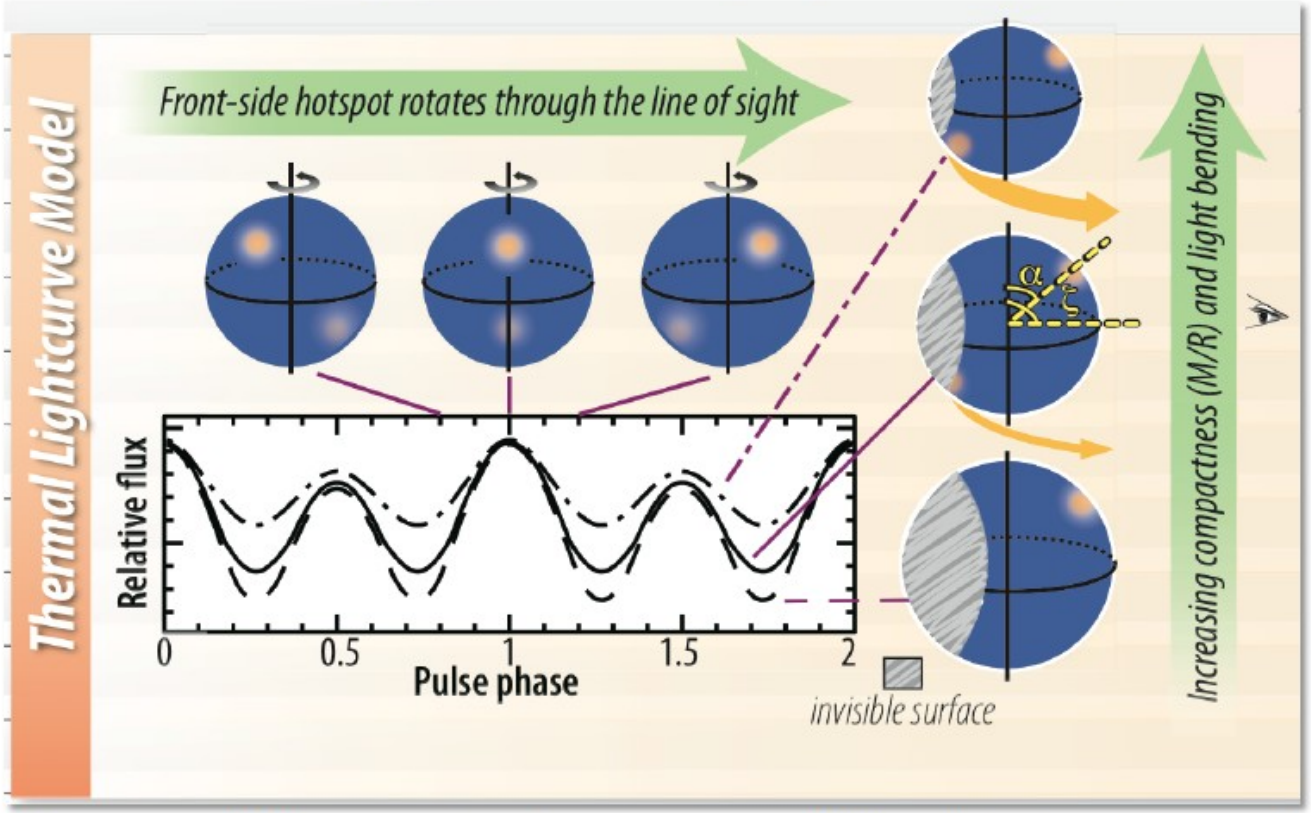

Lightcurve modeling constrains the compactness (M/R) and viewing geometry of a non-accreting millisecond pulsar through the depth of modulation and harmonic content of emission from rotating hot-spots, thanks to gravitational light-bending…

Science Measurements (cont.)

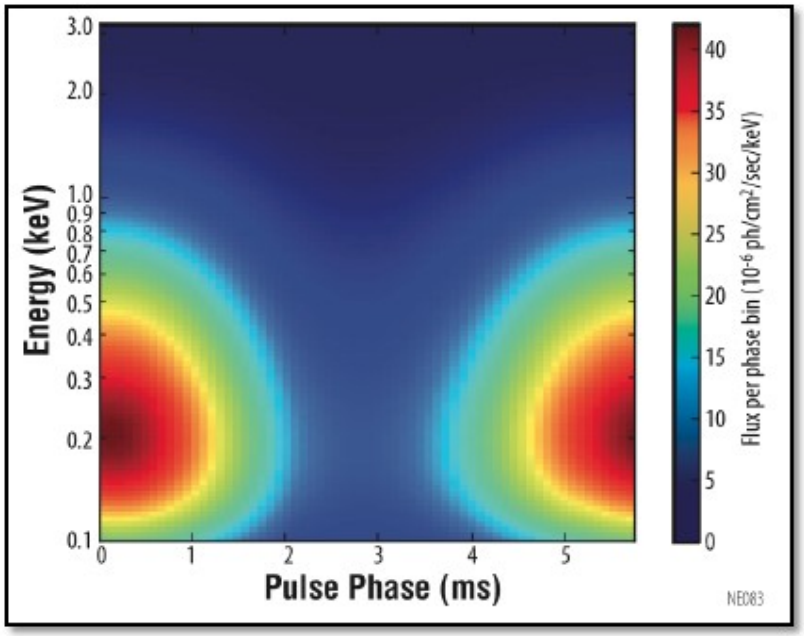

… while phase-resolved spectroscopy promises a direct constraint of radius *R*.

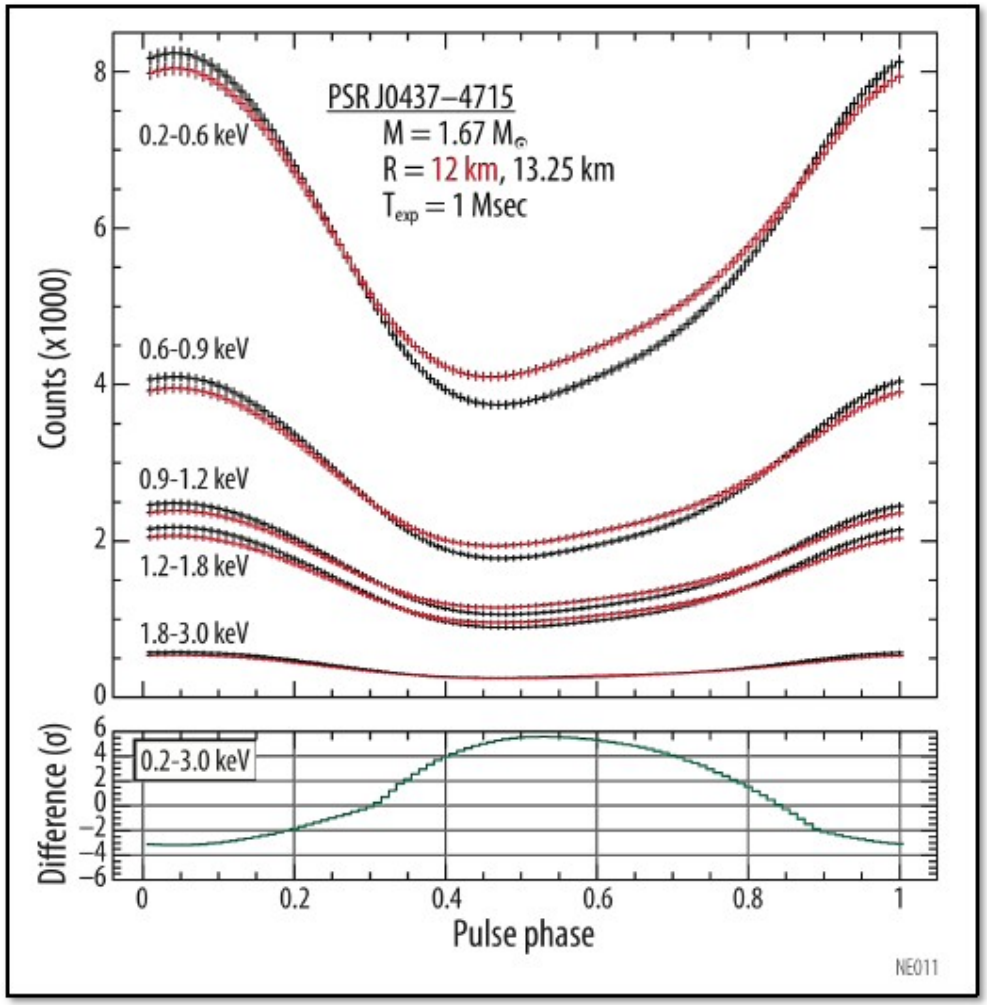

GW170817

- LVC detected a signal consistent with a BNS merger, followed 1.7 s later by a weak gamma-ray burst.
- $\simeq$ 10100 orbits observed over 317 s.
- $\mathcal{M} = 1.186 \pm 0.001\ M_\odot$
- $M_{\rm T,min} = 2^{6/5}\mathcal{M} = 2.725 M_\odot$
- $E_{\rm GW} > 0.025 M_\odot c^2$
- $D_L = 40^{+8}_{-14}$ Mpc
- $75 < \tilde{\Lambda} < 560$ (90%)
- $M_{\rm ejecta} \sim 0.06 \pm 0.02\ M_\odot$
- Blue ejected mass: $\sim 0.01 M_\odot$
- Red ejected mass: $\sim 0.05 M_\odot$
- Probable r-process production
- Ejecta + GRB: $M_{max} \lesssim 2.22 M_\odot$

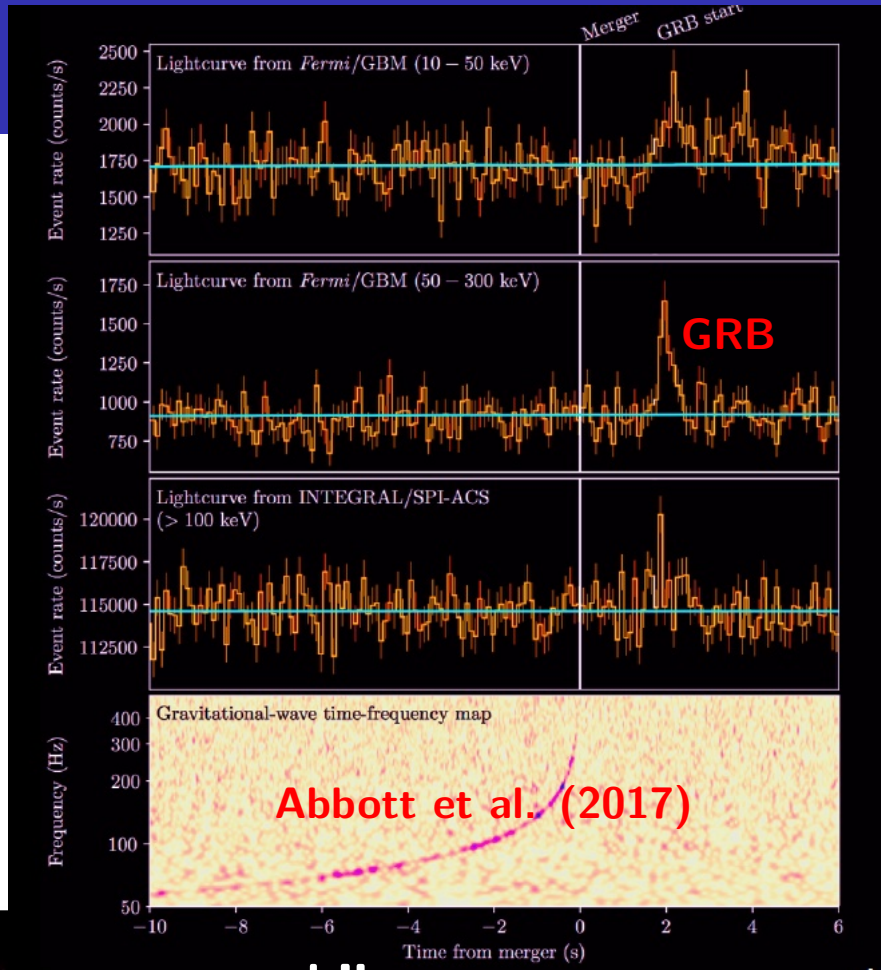

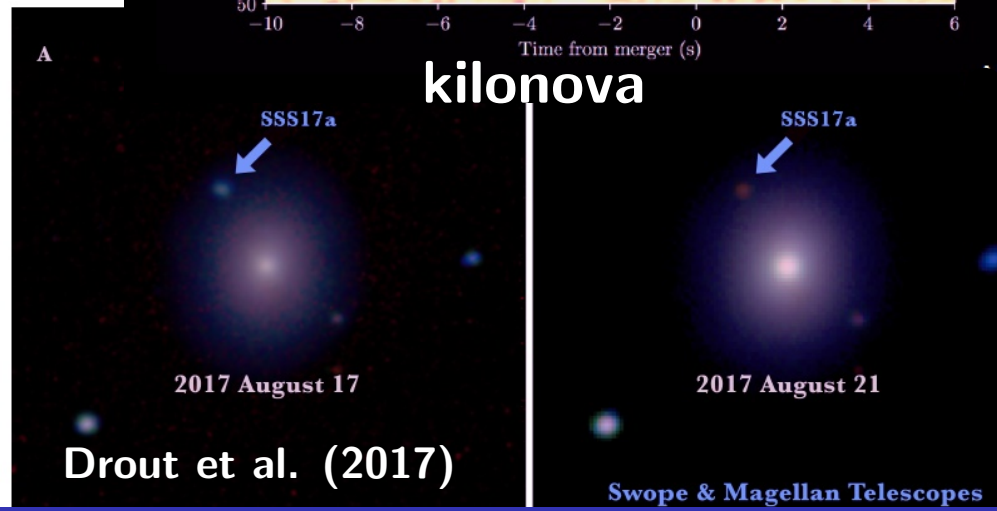

The Effect of Tides

Tides accelerate the inspiral and produce a gravitational wave phase shift compared to the case of two point masses.

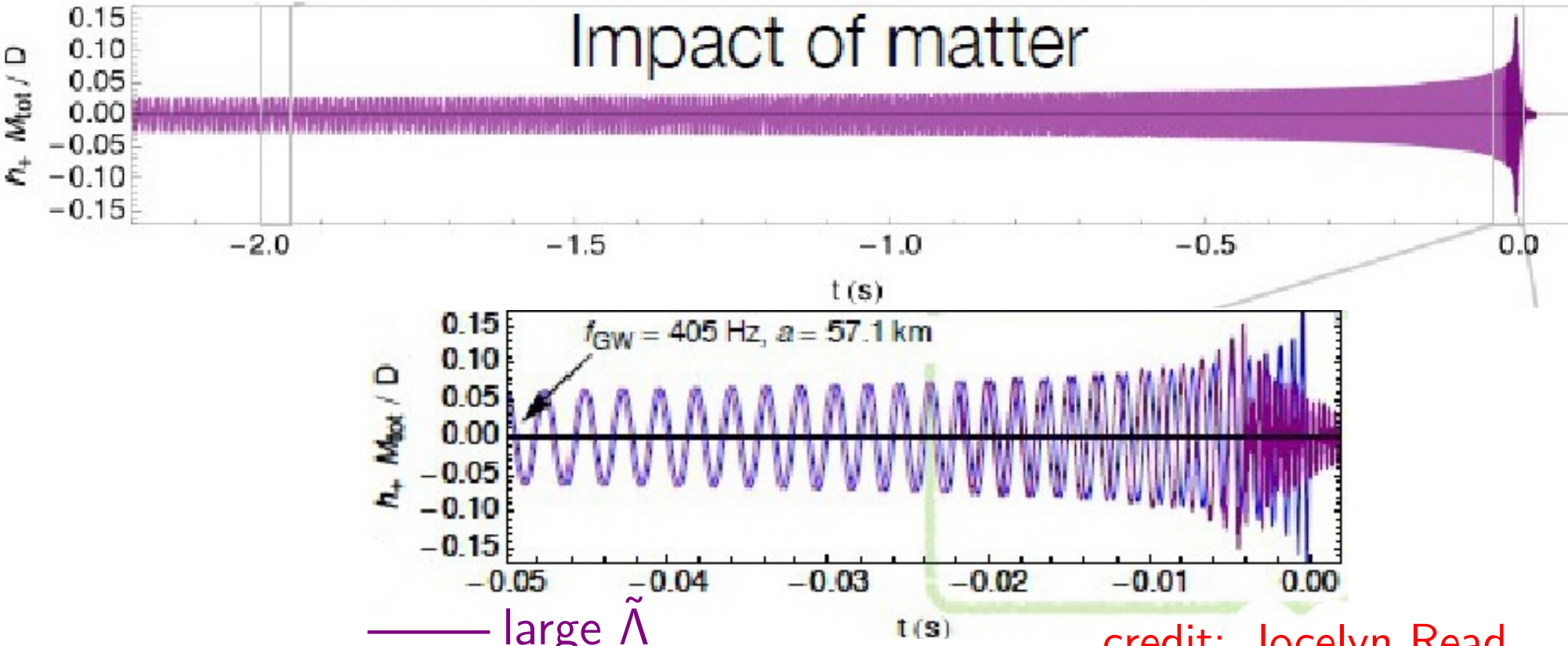

credit: Jocelyn Read

——— large $\tilde{\Lambda}$

——— small $\tilde{\Lambda}$

$$\delta\Phi_t = -\frac{117}{256}\frac{(1+q)^4}{q^2}\left(\frac{\pi f_{GW} G\mathcal{M}}{c^3}\right)^{5/3}\tilde{\Lambda} + \cdots .$$

Tidal Deformability

The tidal deformability λ is the ratio of the induced dipole moment Q_{ij} to the external tidal field E_{ij}, $Q_{ij} \equiv -\lambda E_{ij}$.

Use $\beta = GM/Rc^2$ and

$$\Lambda = \frac{\lambda c^{10}}{G^4 M^5} \equiv \frac{2}{3} k_2 \beta^{-5}.$$

$k_2 \propto 1/\beta$ is the dimensionless Love number, so $\Lambda \simeq a\beta^{-6}$.

For $1 < M/M_\odot < 1.6$, $a = 0.0093 \pm 0.0007$.

For a neutron star binary, the mass-weighted $\tilde{\Lambda}$ is the relevant observable:

$$\tilde{\Lambda} = \frac{16}{13} \frac{(1+12q)\Lambda_1 + (12+q)q^4\Lambda_2}{(1+q)^5},$$

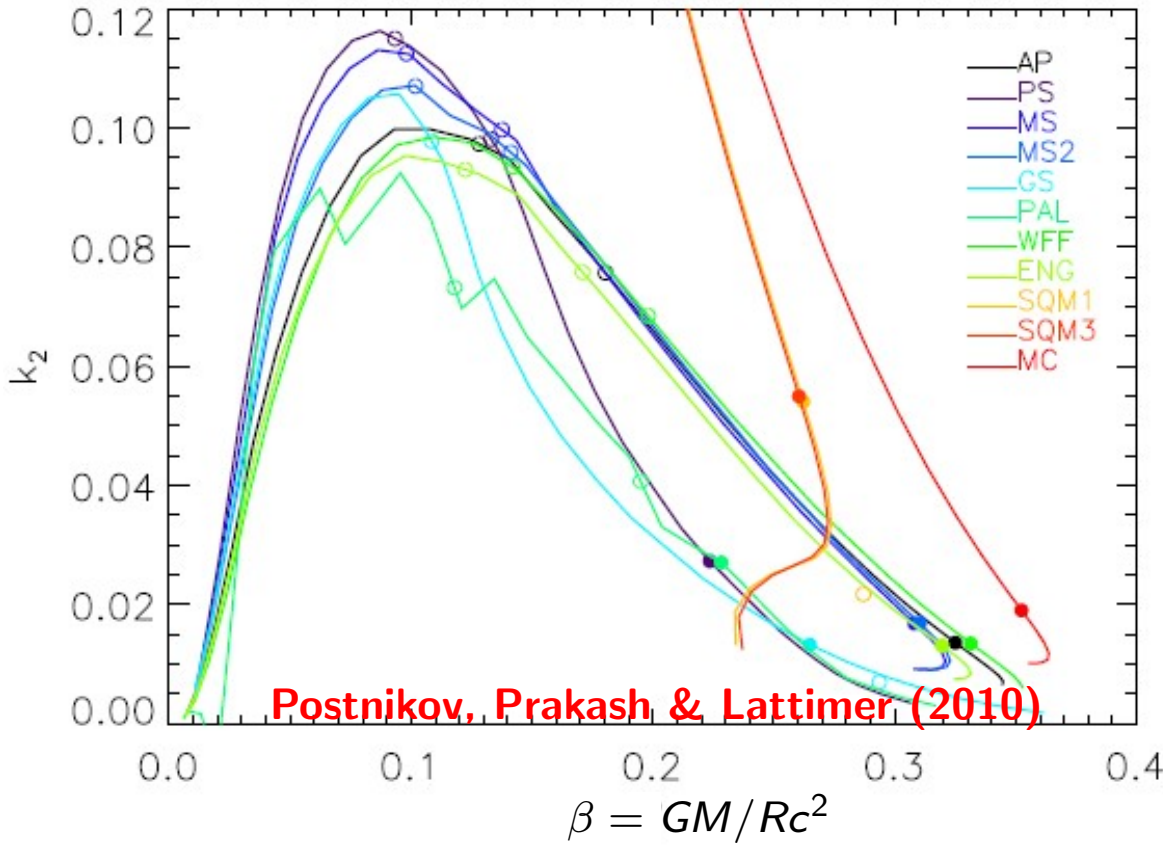

$$q = M_2/M_1 \leq 1$$

Binary Deformability and the Radius

$$\tilde{\Lambda} = \frac{16}{13}\frac{(1+12q)\Lambda_1 + q^4(12+q)\Lambda_2}{(1+q)^5} \simeq \frac{16a}{13}\left(\frac{R_{1.4}c^2}{G\mathcal{M}}\right)^6 \frac{q^{8/5}(12-11q+12q^2)}{(1+q)^{26/5}}.$$

This is very insensitive to q for $q > 0.5$, so

$$\tilde{\Lambda} \simeq a'\left(\frac{R_{1.4}c}{G\mathcal{M}}\right)^6.$$

For $\mathcal{M} = (1.2 \pm 0.2)\ M_\odot$, $a' = 0.0035 \pm 0.0006$,

$$R_{1.4} = (11.5 \pm 0.3)\frac{\mathcal{M}}{M_\odot}\left(\frac{\tilde{\Lambda}}{800}\right)^{1/6} \text{km}.$$

For GW170817, $\mathcal{M} = 1.186 M_\odot$, $a' = 0.00375 \pm 0.00025$,

$$R_{1.4} = (13.4 \pm 0.1)\left(\frac{\tilde{\Lambda}}{800}\right)^{1/6} \text{km}.$$

Implied $\Lambda_{1.4} - L$

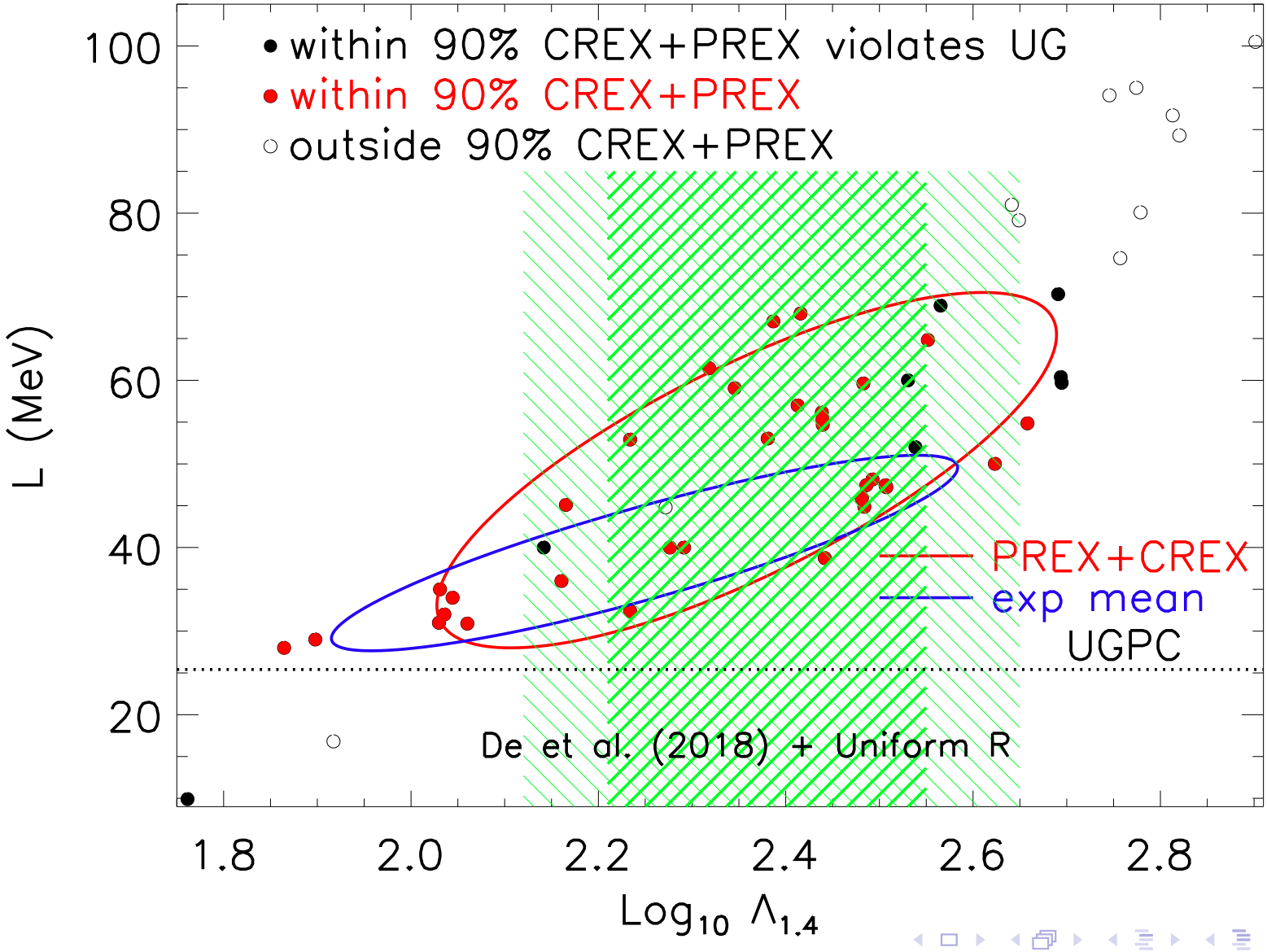

Summary of Astrophysical Observations

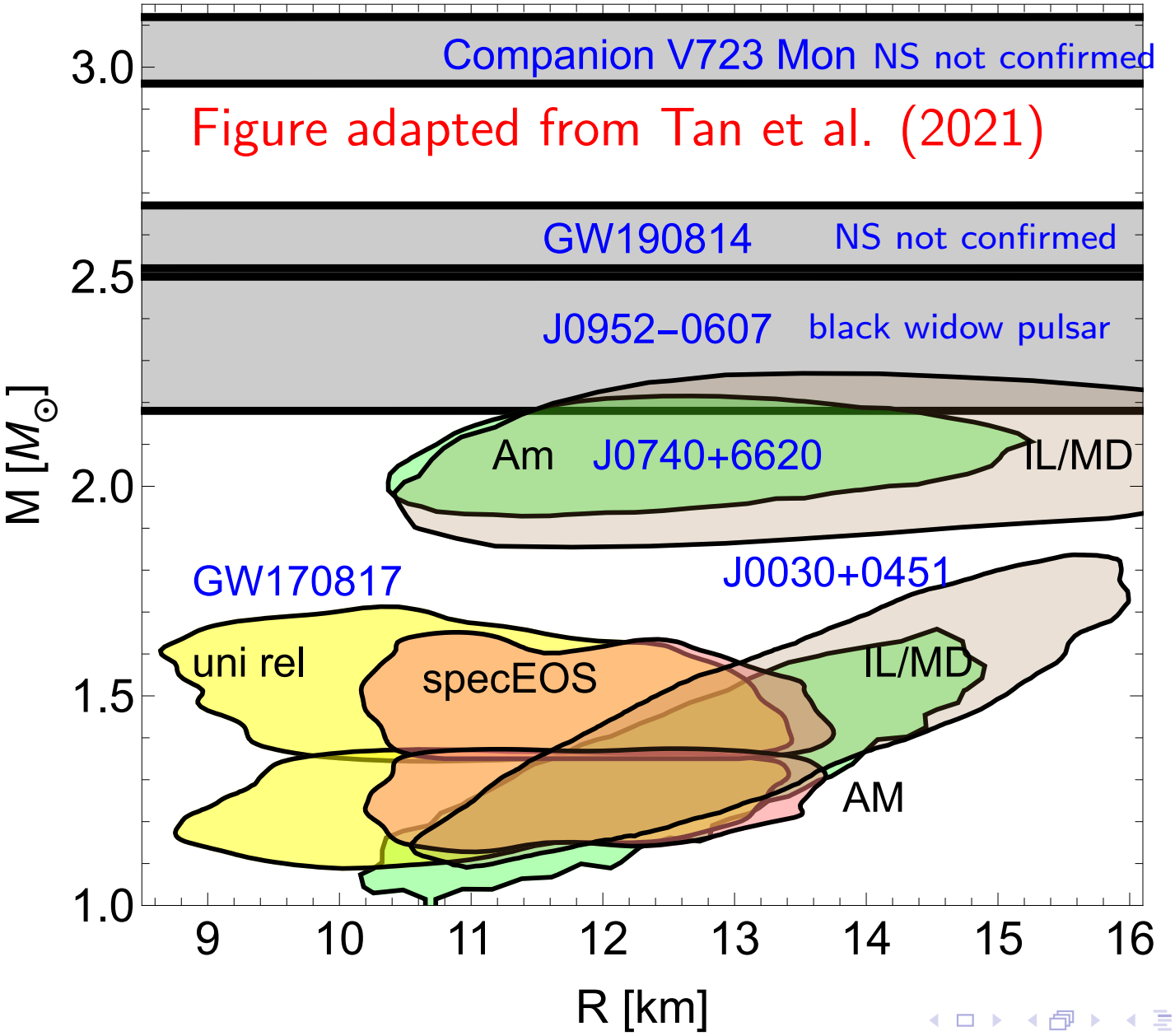

Moment of Inertia

- Spin-orbit coupling is of same magnitude as post-post-Newtonian effects (Barker & O'Connell 1975, Damour & Schaeffer 1988).
- Precession alters orbital inclination angle (observable if system is face-on) and periastron advance (observable if system is edge-on).
- More EOS sensitive than R: $I \propto MR^2$.
- Measurement requires system to be extremely relativistic.
- Double pulsar PSR J0737-3037 is an edge-on candidate; $M_A = 1.338185^{+12}_{-14} M_\odot$.
- Even more relativistic systems are likely to be found, based on faintness and nearness of PSR J0737-3037.

Recent Moment of Inertia Measurement

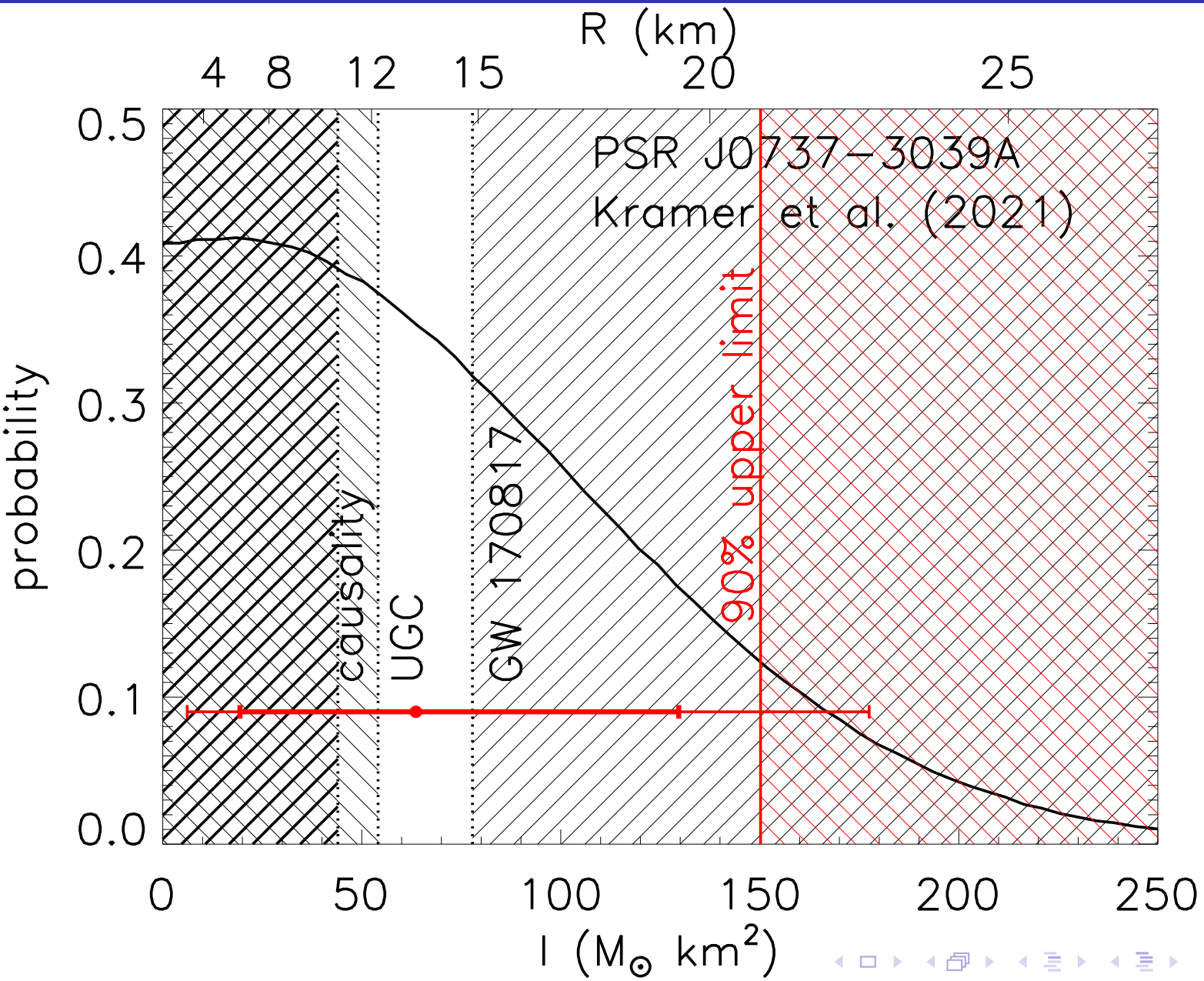

Conclusions

Nuclear experiments and theory, including EDF fits to nuclear binding energies, chiral EFT calculations, and neutron skin and dipole polarizability measurements of ^{48}Ca and ^{208}Pb, consistently predict narrow ranges for the symmetry energy parameters **without any astrophysical inputs**:

$$J = (32 \pm 2)\ \mathrm{MeV}, \quad L = (50 \pm 10)\ \mathrm{MeV}, \quad K_N = (140 \pm 70)\ \mathrm{MeV}.$$

Neutron star radius predictions are about $R_{1.4} = (11.5 \pm 1.0)$ km.

This is consistent with inferences from GW170817, NICER X-ray timing measurements and X-ray observations of quiescent thermal and photospheric radius expansion burst sources.

We eagerly anticipate new neutron skin and dipole polarizability experiments, LIGO/Virgo/Kagra observations of neutron star mergers, radio pulsar timing measurements of masses and moments of inertia measurements, and NICER and other planned X-ray telescope observations of neutron stars.